

Population dynamics, synchrony, and environmental quality of Hokkaido voles lead to temporal and spatial Taylor's laws

JOEL E. COHEN^{1,2,3,5} AND TAKASHI SAITOH⁴

¹Laboratory of Populations, The Rockefeller University and Columbia University, 1230 York Avenue, Box 20, New York, New York 10065-6399 USA

²Department of Statistics, Columbia University, 1255 Amsterdam Avenue, New York, New York 10027 USA

³Department of Statistics, University of Chicago, 5747 South Ellis Avenue, Chicago, Illinois 60637 USA

⁴Field Science Center, Hokkaido University, North-11, West-10, Sapporo 060-0811 Japan

Abstract. Taylor's law (TL) asserts that the variance in a species' population density is a power-law function of its mean population density: $\log(\text{variance}) = a + b \times \log(\text{mean})$. TL is widely verified. We show here that empirical time series of density of the Hokkaido gray-sided vole, *Myodes rufocanus*, sampled 1962–1992 at 85 locations, satisfied temporal and spatial forms of TL. The slopes ($b \pm$ standard error) of the temporal and spatial TL were estimated to be 1.613 ± 0.141 and 1.430 ± 0.132 , respectively. A previously verified autoregressive Gompertz model of the dynamics of these populations generated time series of density which reproduced the form of temporal and spatial TLs, but with slopes that were significantly steeper than the slopes estimated from data. The density-dependent components of the Gompertz model were essential for the temporal TL. Adding to the Gompertz model assumptions that populations with higher mean density have reduced variance of density-independent perturbations and that density-independent perturbations are spatially correlated among populations yielded simulated time series that satisfactorily reproduced the slopes from data. The slopes ($b \pm$ standard error) of the enhanced simulations were 1.619 ± 0.199 for temporal TL and 1.575 ± 0.204 for spatial TL.

Key words: autoregressive time series; density dependence; Gompertz model; population dynamics; rodents; spatial correlation; synchrony; Taylor's law; voles.

INTRODUCTION

Taylor's law (TL; Taylor 1961) is one of the most widely verified empirical rules in ecology (Taylor 1986, Eisler et al. 2008). When applied to a single species, TL asserts that the variance in the population density is a power-law function of its mean population density. The power-law form of TL is written $\text{variance} = a \times (\text{mean})^b$, $a > 0$. Equivalently,

$$\log(\text{variance}) = \log(a) + b \times \log(\text{mean}). \quad (1)$$

The value of b (but not of $\log(a)$) is independent of the base of the logarithms, which we chose to be 10, and of the scale (e.g., individuals/m² vs. individuals/km²) used to measure population density. Both $\log(a)$ and b are estimated by some statistical fitting procedure.

In the temporal TL, the mean and variance are calculated over observations of population density at different times in a given location and one data point ($\log(\text{temporal mean})$, $\log(\text{temporal variance})$) is plotted for each location. In the spatial TL, the mean and variance are calculated over observations of population density in different spatial locations and one data point ($\log(\text{spatial mean})$, $\log(\text{spatial variance})$) is plotted for each time of observation.

Manuscript received 14 December 2015; revised 22 July 2016; accepted 2 August 2016. Corresponding Editor: M. K. Oli.

⁵E-mail: cohen@rockefeller.edu

Many theories and interpretations of TL have been proposed, but none has gained universal or even widespread acceptance. Major questions are: Why TL is so widely observed? What mechanisms or processes generate TL? What can be learned from the values of a and b ? Insufficient progress has been made in answering these questions in part because many previous empirical studies have verified TL without testing the details of any model that leads to TL, while detailed theoretical models that lead to TL have often lacked correspondingly detailed empirical verification of the processes assumed (see reviews by Taylor 1986 and Eisler et al. 2008). One exception (Cohen et al. 2013) showed that a stochastic multiplicative population growth model predicted a spatial TL and that long-term tree censuses in Black Rock Forest, New York, USA, were compatible with the assumptions of the model and the estimated parameters of TL. Although spatial density-dependence has been examined in relation to TL (Taylor et al. 1978), we are not aware that the interaction with TL of temporal density dependence or density independence has been examined previously.

Here we show, first, that empirical time series of population density of a rodent species repeatedly surveyed at multiple locations satisfied temporal and spatial TLs and, second, that a Gompertz autoregressive time-series model, previously demonstrated to describe these populations well (Stenseth et al. 2003), predicted the form and

(under additional assumptions) the empirically estimated slopes of the temporal and spatial TLs. This model represented temporally density-dependent as well as temporally density-independent population regulatory factors. The agreement between the predictions of the Gompertz model and the temporal TL depended primarily on the model's density dependence with 1-yr lag. Adding assumptions of spatial correlation among the density-independent perturbations of the Gompertz model and effects of habitat quality on the variance of density-independent perturbations of the Gompertz model enabled the enhanced model to approximate well the empirically estimated slopes of the temporal and spatial TLs.

The species investigated here, the gray-sided vole [*Myodes rufocanus* (Sundevall, 1846)], was an economically important pest of tree plantations (Kaneko et al. 1998). Rodents are still very important pests for agricultural products in Asia (John 2014). Better understanding via TL of the relation between the mean and the variance of population density offers the possibility to improve the efficiency and precision of pest population estimation and control, as it has for insect pests of soybeans (Kogan et al. 1974, Bechinski and Pedigo 1981) and cotton (Wilson et al. 1989). Better understanding of TL also has important implications for conservation and the interaction between ecology and evolution (Pertoldi et al. 2014).

MATERIALS AND METHODS

Study design and data

Hokkaido is the northernmost island (41°24'–45°31' N, 139°46'–145°49' E) of Japan and covers 78,073 km². The geography of Hokkaido and the data collection have been described (Stenseth et al. 2003). The Forestry Agency of the Japanese Government has investigated vole populations since 1954 in Hokkaido forests covering (as of 1992) 28,400 km². Rodent surveys were carried out twice a year, in spring (May or June) and fall (September or October). Here we analyzed $N = 85$ time series of gray-sided vole populations in the fall covering $T = 31$ years (1962–1992) in the central and northernmost part of Hokkaido (the Asahikawa Regional Office, Forestry Agency of the Japanese Government; Saitoh et al. 1997), because this regional office provided the longest data sets. Fall data represented better inter-annual fluctuations because they varied more than spring data.

A basic unit of the rodent survey was 150 trap-nights, which consisted of 50 snap traps set at 10-m intervals on 0.5 ha of land for three consecutive nights (Saitoh et al. 1997, 1998). We defined vole population density as the number of voles captured per 150 trap-nights. The raw data $M_{t,j}$, the total number of trapped voles in a ranger office which carried out the rodent survey on several plots (which yielded several units of 150 trap-nights), are presented as DataS1.zip Appendix 1 in a $T \times N$ matrix with

$T = 31$ rows, one for each year $t = 1962, 1964, \dots, 1992$, and $N = 85$ columns, $j = 1, 2, \dots, 85$, one for each ranger office. The amount of trapping effort (trap-nights) is given in DataS1.zip Appendix 2. There were no missing values.

Statistical procedures

The traditional frequentist (or Fisher) estimates of population density (per 150 trap nights) were (counts of voles $M_{t,j}$ in year t at site j)/(number of trap nights in year t at site $j/150$). All actual trapping efforts (actual number of trap nights) were ≥ 150 trap nights.

We then used WinBUGS version 1.4.3 (Spiegelhalter et al. 2003) for Bayesian analysis using Markov chain Monte Carlo methods to produce Bayesian (or “Bayes”) estimates of population density (per 150 trap nights) for each year and study site. These Bayes estimates take account of trapping effort and assume Poisson variation in actual counts, given an expected mean. In brief, Bayesian estimates adjust each frequentist estimate (usually very slightly) by “borrowing strength” from the distribution of the full array of data, often (as here) reducing the effects of outliers. The resulting Bayes population estimates are presented in DataS1.zip Appendix 3 in a $T \times N$ matrix $N_{t,j}$ with 31 rows, one for each year, and 85 columns, one for each study site. All $N_{t,j} > 0$.

We compared the Fisher and Bayes estimates of population density, site by site, year by year. For low counts, Fisher and Bayes agreed closely, but when the Fisher counts exceeded about 35 voles per 150 trap nights, Bayes counts tended to be slightly less than Fisher counts (Appendix S1: Fig. S1A). The temporal mean of Fisher counts agreed very closely with the temporal mean of Bayes counts (Appendix S1: Fig. S1B) and likewise for the spatial means (Appendix S1: Fig. S1C). However, the estimates of the spatial and temporal variances from Bayes were systematically slightly lower than those from Fisher (Appendix S1: Fig. S1D, E).

Neither the Fisher nor the Bayes estimates takes account of possible differences in observability of voles at different sites or in different years.

Sample estimates of the variance are highly variable when, as here, the number of observations is limited. Therefore we accepted the Bayes estimates of mean and variance as more reliable and used them in all subsequent analyses. By providing the raw data on which Bayes estimates are based, we enable anyone to do independent analyses of the counts and sampling efforts.

Gompertz model

For each population j , using the Bayesian estimates of $N_{t,j}$ in $x_{t,j} = \log_e(N_{t,j}) = 2.302585 \times \log_{10}(N_{t,j})$, we calculated the temporal mean of $x_{t,j}$, namely $\bar{x}_j = (1/31) \sum_{t=1962}^{1992} x_{t,j}$, which is the natural logarithm of the geometric mean over time of $N_{t,j}$, and then subtracted \bar{x}_j from the time series of $x_{t,j}$ to get the centered time series $y_{t,j} = x_{t,j} - \bar{x}_j$ for population j . Thus $y_{t,j}$ is the natural logarithm of $N_{t,j}$ divided by

the geometric mean over time of $N_{t,j}$. Then we fitted the Gompertz model, a homogeneous (no constant term) second-order autoregressive model to $y_{t,j}$

$$y_{t,j} = (1 + a_{1,j})y_{t-1,j} + a_{2,j}y_{t-2,j} + e_{t,j} \quad (2)$$

where the j th population's coefficient of density dependence for a 1-yr lag is $a_{1,j}$ and for a 2-yr lag is $a_{2,j}$. The error term $e_{t,j}$ represents density-independent effects. It is modeled by a normal distribution with mean equal to 0 and a standard deviation SD_j that is constant in time but may differ from one population j to another.

Instead of modeling process and observation separately, we used WinBUGS to obtain Bayesian estimates of $a_{1,j}$, $a_{2,j}$, and SD_j taking sampling error into consideration (WinBUGS code is in DataS1.zip Appendix 5). The median of the posterior distribution was used for each parameter estimate. We also estimated those parameters using Yule-Walker estimation as coded in the aryule.m function in the Signal Processing Toolbox of Matlab (MathWorks 2015) (results in DataS1.zip Appendix 3).

The Gompertz model (Eq. 2) can describe various fluctuation patterns of population dynamics (Royama 1992) and is commonly applied to analyses of vole populations (Stenseth et al. 1996, 1998, Saitoh et al. 1997, 1998). But the Gompertz model does not explicitly link a_1 and a_2 to underlying demographic processes of birth, death, and migration. Hence it is not yet possible to interpret a_1 and a_2 in terms of these processes. Despite numerous analyses of cyclic patterns in vole populations, how demographic processes control rodent population cycles remains hypothetical (Andreassen et al. 2013). While the rates of the reproduction and survival of Hokkaido voles are expected to be negatively affected by higher density, the relative importance of these demographic components of population change in explaining annual population fluctuations remains unclear. Quantitative information on the magnitudes and population-dynamic consequences of immigration and emigration is very limited.

Nevertheless, values of a_1 and a_2 can be interpreted, on a relative basis, in terms of ecological density dependence or density independence. Specifically, a_1 represents a return tendency to an equilibrium density (density dependence in a narrow sense) and populations with more negative values are less variable, while a_2 generates variability for a population and populations with more negative values are more likely to be cyclic (Royama 1992). Density dependence with a 1-yr lag is strong and prevalent in populations of the Hokkaido vole (Saitoh et al. 1997, 1998, Stenseth et al. 2003).

Simulations

We generated three simulations using progressively stronger assumptions which were demanded by our progressively deeper understanding of the data: the so-called Fundamental simulations, the Adjusted SD simulations, and the Synchronized e_t simulations. The state variable in all simulations was the centered log-transformed

population density $y_{t,j} = x_{t,j} - \bar{x}_j$. The values of $y_{t,j}$ generated by each simulation were then transformed back to the original scale of population density using the observed temporal sample means \bar{x}_j , and then the means and variances that appear in the tests of TL were computed from these reverted values.

The Fundamental simulation used the Gompertz model (Eq. 2) with the population-specific estimates of $a_{1,j}$ and $a_{2,j}$ and SD_j to generate 85 time series corresponding to 85 observed populations. The initial two observed centered log-transformed values $y_{1,j}$, $y_{2,j}$ were used for the first two values of each simulated population. The length of every simulated time series was 31 yr, the same as observed.

We also did two additional simulations. The Adjusted SD simulations differed from the Fundamental simulation only in replacing SD_j by the estimated $SD_j - (0.174 \times 2.302585 \times \log_{10}(\text{estimated temporal mean } \bar{x}_j))$ for each j . The empirical basis for this adjustment is described in *Results* and its ecological rationale and interpretation are explained in the *Discussion*.

To generate the Synchronized e_t simulations, we first generated a fixed baseline error time series $e_{t,0}$ of 31 independent and identically distributed normal random numbers with mean 0 and SD 1. Then we generated 85 correlated time series $e_{t,j}$, $j = 1, \dots, 85$, of length 31 years ($t = 1, \dots, 31$), using the formula $e_{t,j} = \rho \times e_{t,0} + (1 - \rho^2)^{1/2} \times \mathcal{N}_{t,j}(0, 1)$, where $\mathcal{N}_{t,j}(0, 1)$ are independent and identically distributed normal random numbers with mean 0 and SD 1. Consequently, the correlation over time between the error terms of any two simulated time series, for example, $e_{t,1}$ and $e_{t,2}$, would be ρ^2 if the time series were infinitely long. We examined the effect of ρ on the simulated spatial TL by an Approximate Bayesian Computation method (Csilléry et al. 2012). This procedure was a numerical search for the level of spatial correlation of population dynamics that gave the best agreement between the log(mean) and log(variance) of simulations and the log(mean) and log(variance) on the original scale of measurement of population density.

Temporal Taylor's law

For each population $j = 1, 2, \dots, 85$, separately, we calculated the sample mean $\bar{N}_j = (1/31) \sum_{t=1962}^{1992} N_{t,j}$ of Bayesian estimated population density $N_{t,j}$ over time (temporal sample mean) and the sample variance over time (temporal sample variance) $(1/30) \sum_{t=1962}^{1992} (N_{t,j} - \bar{N}_j)^2$ of the j th time series of 31 Bayesian estimates of the number of voles per 150 trap-nights ($N_{t,j}$; $t = 1962, 1963, \dots, 1992$) in R (DataS1.zip Appendix 3). We defined

$$X(\text{population } j) = \log_{10}(\text{temporal sample mean of } N_{t,j}),$$

$$Y(\text{population } j) = \log_{10}(\text{temporal sample variance of } N_{t,j}).$$

We used ordinary least-squares regression (OLS) to fit Eq. 1 to these 85 values of $X(\text{population } j)$ and

$Y(\text{population } j)$. The use of OLS to fit log-log transformed versions of power laws has been criticized (Tokeshi 1995, Packard 2009, Packard et al. 2011). Strictly speaking, the use of OLS is invalid when observation errors are included in the abscissa, and here every observation of $X(\text{population } j)$ is subject to sampling variability. However, the use of OLS in fitting TL is recommended (Xiao et al. 2011, Lai et al. 2013) because the sampling variability of $X(\text{population } j)$ is much smaller than the sampling variability of $Y(\text{population } j)$, and numerous practical evaluations of using OLS to fit TL suggest that it gives reasonable results. Therefore we used OLS.

To test for nonlinearity in the relation between $Y(\text{population } j)$ and $X(\text{population } j)$, we used OLS to fit a quadratic generalization of TL (due to Taylor et al. 1978: Eq. 14): $Y(\text{population } j) = \log(a) + b \times X(\text{population } j) + c \times [X(\text{population } j)]^2$. We accepted TL as an approximate representation of the relationship of temporal sample variance to temporal sample mean if c in the quadratic model did not differ significantly from zero and the slope b in the linear model, Eq. 1, differed significantly from zero.

All regressions were computed using function `lm` in R version 3.2.2. The critical value for statistical significance was always $P = 0.05$ without any correction for multiple inferences.

Spatial Taylor's law

For each year $t = 1962, 1963, \dots, 1992$, separately, we calculated the sample mean $\bar{N}_t = (1/85) \sum_{j=1}^{85} N_{t,j}$ of Bayesian estimated population density $N_{t,j}$ (spatial sample mean) and the sample variance $(1/84) \sum_{j=1}^{85} (N_{t,j} - \bar{N}_t)^2$ (spatial sample variance) over the 85 populations $j = 1, \dots, 85$ (DataS1.zip Appendix 3). We defined

$$X(\text{year } t) = \log_{10}(\text{spatial sample mean of } N_{t,j})$$

$$Y(\text{year } t) = \log_{10}(\text{spatial sample variance of } N_{t,j}).$$

Using the same procedure as for the temporal TL, we fitted Eq. 1 and tested for nonlinearity by fitting a quadratic generalization of TL.

Factors influencing Taylor's law

The simulations of the Gompertz model are determined by three parameters (a_1 , a_2 , and SD) and the estimated mean of empirical densities. Since more negative a_1 represents a stronger force to return densities to equilibrium, higher values of a_1 are predicted to increase the variance of densities. Since populations with more negative values of a_2 are more likely to be cyclic (Royama 1992), higher values of a_2 are predicted to decrease the variance of densities. Since SD determines the degree of density-independent disturbance, higher values of SD are predicted to increase the variance of densities.

We analyzed the effects of the parameters of the Gompertz model on the variance and mean of the

empirical and simulated densities by means of generalized linear model (GLM) analyses with the three parameters as explanatory variables and the log(variance) and log(mean) of empirical and simulated densities as separate response variables. If the Gompertz model sufficiently captured the population dynamics, the GLM analyses would be expected to yield similar results when comparing empirical and simulated time series.

In addition, if a parameter consistently affects both variance and mean, that parameter is considered to contribute to the formation of TL. For example, if a factor X is linearly related to both log(variance) and log(mean), i.e., if X satisfies $\log(\text{variance}) = r + s \times X$ and $\log(\text{mean}) = u + v \times X$, $v \neq 0$, then TL must be true. Why? Solving for X in the second equation gives $X = [\log(\text{mean}) - u]/v$ and then the first equation gives $\log(\text{variance}) = r + s \times [\log(\text{mean}) - u]/v = (r - s \times u/v) + (s/v) \times \log(\text{mean})$. This linear relationship between log(variance) and log(mean) is TL with intercept $r - s \times u/v$ and slope s/v . If the signs of s and v are same (both are negative or positive), that factor X contributes to forming a positive slope of TL. If the signs of s and v are different, that factor X leads towards a negative slope of TL.

RESULTS

Basic features of population fluctuation

Densities fluctuated with 2–5-yr periods (Fig. 1A). In some years most populations showed a peak or a trough of density. For example, $\log_{10}(\text{densities})$ of 61 populations (71.8%) were lower than 0.5 in 1975, while those of 67 populations (78.8%) were higher than 1.0 in 1978. The range of \log_{10} spatial mean densities was 0.273–1.316 for 85 populations. Like spatial mean densities, the \log_{10} spatial variance of densities also fluctuated over time, ranging between 0.739 and 2.264. As a function of year t , the spatial means and spatial variances showed no pronounced or statistically significant trends (slope = -0.004 , $t = -0.800$, $P = 0.430$, adjusted $R^2 = -0.012$ for the mean; slope = -0.004 , $t = -0.510$, $P = 0.614$, adjusted $R^2 = -0.025$ for the variance).

The 85 observed populations were generally pairwise correlated over time but the extent (even the sign) of the correlation varied widely. The mean of the 3570 pairwise correlation coefficients ($3570 = 85 \times 84/2$) of population density measured by the Bayesian adjusted population density was 0.297 ± 0.202 (SD). The maximum pairwise correlation was 0.902 and the minimum was -0.378 . The correlation coefficients were significantly higher than zero in 1,392 pairs (39.0%).

A linear regression of the pairwise correlation on the \log_{10} of pairwise Euclidean distance [range 3,645–226,970 m] between each pair of populations had slope \pm standard error = -0.228 ± 0.011 ($P \approx 2 \times 10^{-16}$) but the adjusted $R^2 = 0.1071$ was not high. These results indicate that nearer populations had more closely correlated

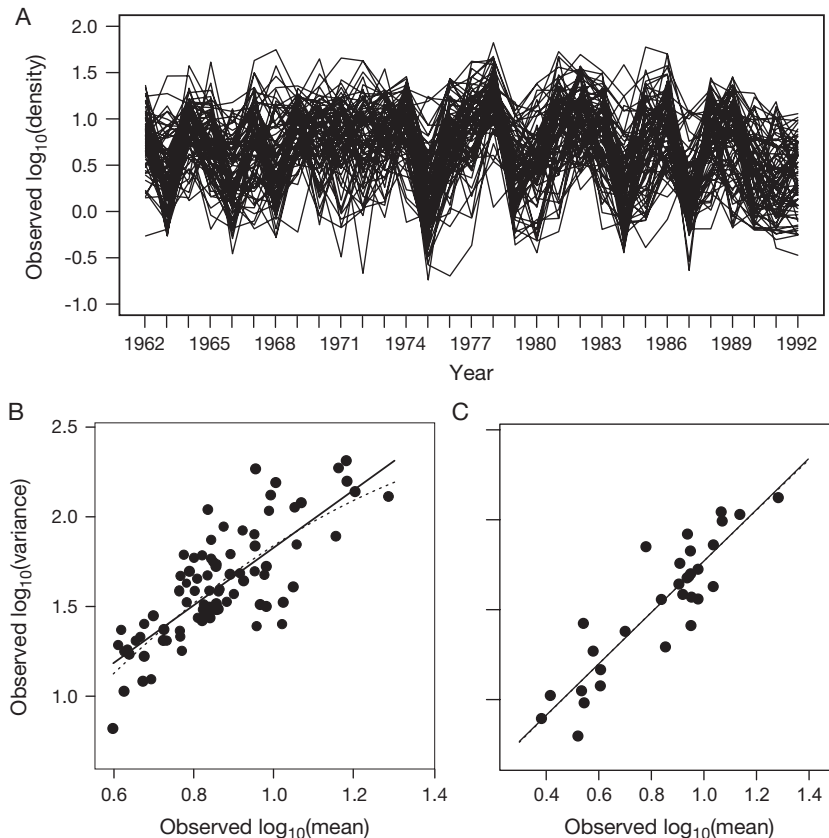


FIG. 1. (A) Observed time series of the \log_{10} Bayesian estimate of population density $N_{t,j}$ of 85 gray-sided vole populations in Hokkaido, Japan in 1962–1992. (B) Test of temporal Taylor's law (TL) for population density. The straight solid line is the least-squares linear regression of $\log_{10}(\text{temporal variance})$ as a function of $\log_{10}(\text{temporal mean})$ for observed populations. The curved dotted line is the least-squares quadratic regression. (C) Test of spatial TL for population density. Straight solid and curved dotted lines are as in (B) for spatial variance and spatial mean. The curved dotted line is almost hidden by the straight solid line because the quadratic coefficient is very small and the other coefficients are almost identical to those of TL. Parameter estimates for linear and quadratic regressions in (B) and (C) are given in Appendix S1: Table S1.

population dynamics but other factors in addition to distance evidently affected the correlation of population dynamics.

Temporal and spatial Taylor's laws

We tested TL by using the Bayesian estimates $N_{t,j}$ of population density, *not* log-transformed and *not* centered, but on the original scale of measurement, to calculate the temporal and spatial variances and means.

TL described adequately the relation of $Y(\text{population } j) = \log(\text{temporal variance})$ of population density to $X(\text{population } j) = \log(\text{temporal mean})$ of population density (Fig. 1B), with slope $b \pm$ standard error = 1.613 ± 0.141 and adjusted $R^2 = 0.607$ (Appendix S1: Table S1). Quadratic regression revealed no statistically significant evidence of nonlinearity.

TL described the relation of $Y(\text{year } t) = \log(\text{spatial variance})$ of population density to $X(\text{year } t) = \log(\text{spatial mean})$ of population density (Fig. 1C), with slope $b \pm$ standard error = 1.430 ± 0.132 and adjusted $R^2 = 0.795$

(Appendix S1: Table S2), a tighter linear relationship than the temporal TL. Quadratic regression revealed no statistically significant evidence of nonlinearity.

Do simulations of the Gompertz model obey a temporal Taylor's law?

In the Fundamental simulations, $\log(\text{temporal variance})$ of density was linearly related to $\log(\text{temporal mean})$ of density (Fig. 2A) with slope $b \pm$ standard error = 2.699 ± 0.214 (Appendix S1: Table S3). Quadratic regression revealed no statistically significant evidence of nonlinearity. In comparison with the observed populations, Fundamental simulated populations showed a significantly steeper slope of TL (Appendix S1: Table S3; ANCOVA, $t = 4.054$, $P < 0.001$). Although the $\log(\text{temporal mean})$ of both observed populations and Fundamental simulations fell in the range from roughly 0.6 to 1.3 (that is, roughly $4 = 10^{0.6}$ to $20 = 10^{1.3}$ voles per 150 trap-nights), the $\log(\text{temporal variance})$ of observed populations ranged from roughly 0.8 to 2.3 (Fig. 1C)

while the log(temporal variance) of Fundamental simulations ranged from roughly 1.0 to 4.0 (Fig. 2A), a range twice as wide.

In GLM analyses of the effects of the Gompertz parameters on the temporal variance of densities, a_1 and SD showed positive effects on the temporal variance while a_2 had negative effects, for both the empirical and the Fundamental simulated densities, as predicted (Table 1). The effects of SD only (not a_1 and a_2) were statistically significant. In contrast, the GLM had very small, and statistically insignificant, adjusted R^2 for the model of the temporal mean of the empirical and Fundamental simulated densities, so the Gompertz parameters did not explain variations in the temporal mean, empirical or Fundamental simulated.

When SD (alone) was regressed on the empirical temporal mean densities, we found $SD = 1.384 - 0.174 \times \log_e(\text{temporal mean})$, with $R^2 = 0.043$, $F_{1,83} = 4.743$, $P = 0.032$. Using this relationship between SD and the empirical temporal mean in the simulations, we adjusted SD using the following equation: Adjusted SD = estimated SD of the empirical densities $- 0.174 \times \log_e(\text{temporal mean of empirical densities})$. For these Adjusted SD simulations, a clear linear relation was observed between log(temporal variance) of density and log(temporal mean) (Fig. 2D), and every parameter of the regression of the simulated log(temporal variance) as a function of the simulated log(temporal mean) was similar to that for the temporal TL for observed populations (for Adjusted SD simulations: slope $b \pm$ standard error = 1.671 ± 0.321 and adjusted $R^2 = 0.237$; see also Appendix S1: Table S4; ANCOVA, $P > 0.6$). Both log(temporal mean) and log(temporal variance) of density showed good agreements between observed populations and the Adjusted SD simulations (Fig. 2E and F; Appendix S1: Table S4).

Do simulations of the Gompertz model obey a spatial Taylor's law?

Using exactly the same time series produced by Adjusted SD simulations that realistically approximated the temporal TL, we tested whether the Gompertz model could simulate the observed spatial TL (Fig. 1C). The simulated log(spatial variance) of density was a linear function of the simulated log(spatial mean) of density, but with significant evidence of nonlinearity (Appendix S1: Table S5). The slope $b \pm$ standard error = 3.283 ± 0.464 was significantly steeper than the slope of the observed TL (Appendix S1: Table S5; ANCOVA, $t = 4.109$, $P = 0.001$).

The pairwise correlation over time of the 85 time series (corresponding to 85 spatial locations) produced by the Adjusted SD simulation was low, as expected, since independent error terms were used for each population and each year. The mean of the correlation coefficients, 0.013 ± 0.183 (SD), was significantly lower than the mean of the pairwise correlations of the observed 85 populations (t test, $t = 40.050$, $P < 0.001$). The percentage of

positive significant correlations for the Adjusted SD simulation (4.7%) was very close to the value expected by chance, as expected.

To examine whether the lack of spatial correlation in the Adjusted SD simulation might be responsible for the difference in the spatial TL between the observed populations and the Adjusted SD simulations, correlated time series were generated by using spatially (not temporally) correlated $e_{t,j}$ (Methods). When $\rho = 0.617$, the Synchronized e_t simulations' time series produced a most likely set of time series that satisfied both TLs. The mean of the spatially pairwise correlations over time in the Synchronized e_t simulations was 0.201, not so different from the mean of the spatially pairwise correlations over time in the observed populations (0.297). In the Synchronized e_t simulations, the log(spatial variance) of density was linearly related to log(spatial mean) of density (Fig. 3D), with slope $b \pm$ standard error = 1.575 ± 0.204 . No significant differences were found in the slope and the intercept between the observed populations and the Synchronized e_t simulations (Appendix S1: Table S6; ANCOVA, $P > 0.5$). However, the log(spatial mean) and log(spatial variance) of density did not show tight agreement between observed populations and the Synchronized e_t simulations (Fig. 3E and F; Appendix S1: Table S6). Quadratic regression did not show any statistically significant evidence of nonlinearity (Appendix S1: Table S6) in the relation of the Synchronized e_t simulated variance to the Synchronized e_t simulated mean.

The Synchronized e_t simulation also showed a clear temporal TL (Fig. 3A), with slope $b \pm$ standard error = 1.619 ± 0.199 . No significant differences were found in the slope and the intercept between the observed populations and the Synchronized e_t simulations (Appendix S1: Table S7; ANCOVA, $P > 0.4$). Both log(temporal mean) and log(temporal variance) of density showed relatively good agreements between observed populations and the Synchronized e_t simulation (Fig. 3B and C; Appendix S1: Table S7).

The same simulation analyses were carried out using the parameters estimated by the Yule-Walker method. They provided results resembling those from the Bayesian estimates. The Fundamental simulation provided the form of temporal and spatial TLs, but with slopes that were significantly steeper than the slopes estimated from the data (Appendix S1: Tables S8–S12). The Synchronized e_t simulation generated simulated time series that satisfied both the temporal TL with slope $b \pm$ standard error = 1.794 ± 0.172 and the spatial TL with slope $b \pm$ standard error = 1.540 ± 0.251 through the Adjusted SD simulation (Appendix S1: Tables S11 and S12, Fig. S2).

DISCUSSION

Empirical results on Taylor's law

In populations of gray-sided voles surveyed at 85 sites in Hokkaido, Japan, from 1962 through 1992, the

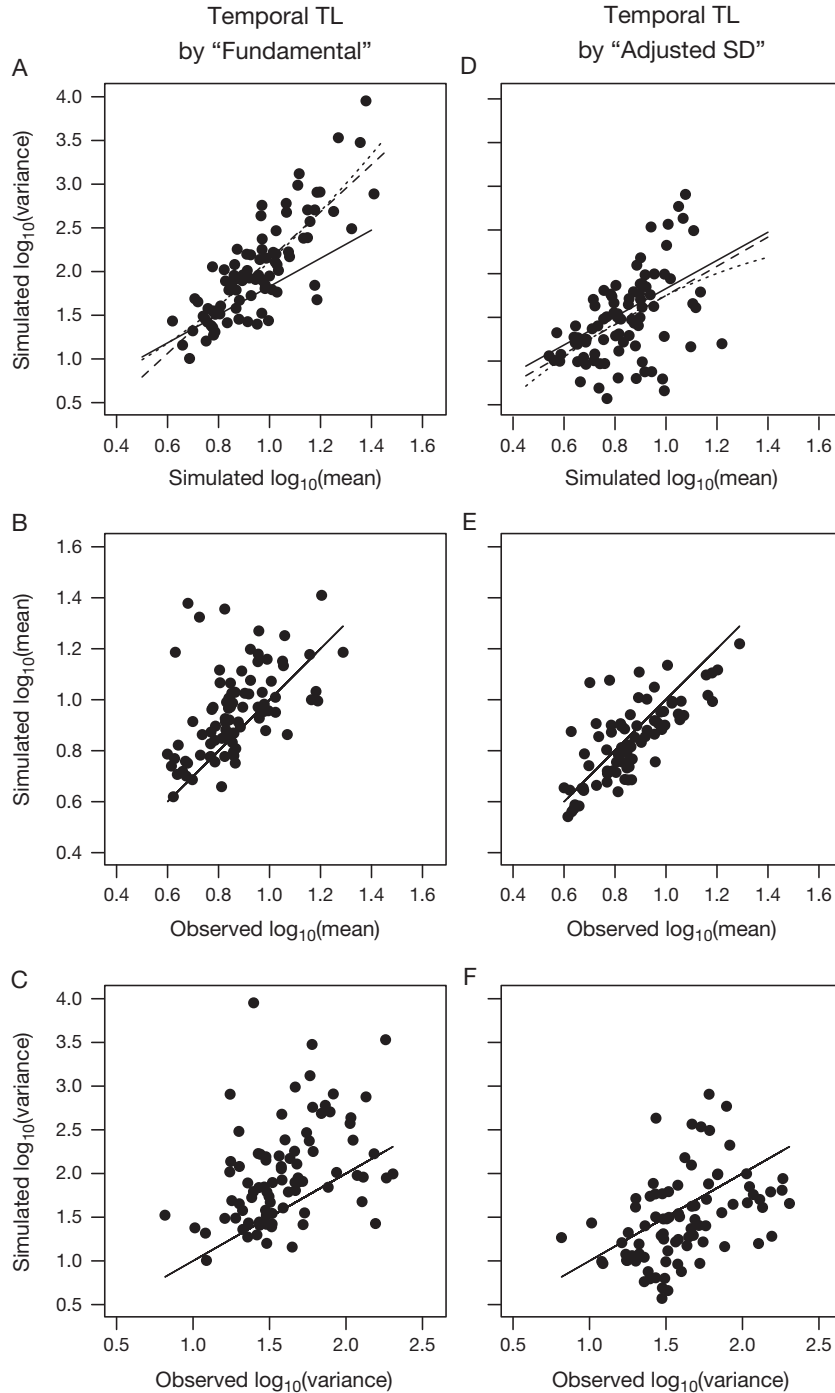


FIG. 2. The temporal TLs, temporal means, and the temporal variances of population density in the Fundamental simulation (A, B, and C) and the Adjusted SD simulation (D, E, and F) (85 time series, each lasting 31 years). (A) Temporal TLs: $\log_{10}(\text{temporal variance})$ as a function of $\log_{10}(\text{temporal mean})$ for Fundamental simulations using observed $a_{1,j}$, observed $a_{2,j}$, and observed SD_j . (D) $\log_{10}(\text{temporal variance})$ as a function of $\log_{10}(\text{temporal mean})$ for Adjusted SD simulations using observed $a_{1,j}$, observed $a_{2,j}$, and adjusted SD_j . Solid line is the ordinary least squares (OLS) regression for observed populations. The broken and dotted lines represent the linear and quadratic relationship in these simulations, respectively. (B and E) Simulated $\log_{10}(\text{temporal mean density})$ as a function of empirical $\log_{10}(\text{temporal mean density})$ in the Fundamental (B) and Adjusted SD (E) simulations. The solid line represents $y = x$. (C and F) Simulated $\log_{10}(\text{temporal variance of density})$ as a function of empirical $\log_{10}(\text{temporal variance of density})$ in the Fundamental (C) and Adjusted SD (F) simulations. The solid line represents $y = x$.

TABLE 1. Partial regression coefficient estimates (PRC), standard error (SE), *t* value, and standardized partial regression coefficients (β) of explanatory variables in the generalized linear model for temporal variance and temporal mean on empirical densities and simulated densities.

Parameter	PRC	SE	<i>t</i>	β
a) Variance of empirical densities (Adj. $R^2 = 0.061$; $F_{3,81} = 2.839^*$)				
a_1	0.191	0.133	1.438	0.161
a_2	-0.135	0.113	-1.202	-0.136
SD	0.291	0.128	2.279*	0.243
Intercept	1.277	0.136	9.397***	NA
b) Variance of simulated densities (Adj. $R^2 = 0.311$; $F_{3,81} = 13.63^{***}$)				
a_1	0.089	0.216	0.411	0.040
a_2	-0.149	0.183	-0.815	-0.079
SD	1.285	0.207	6.202***	0.566
Intercept	0.600	0.221	2.994**	NA
c) Mean of empirical densities (Adj. $R^2 = 0.038$; $F_{3,81} = 2.114$)				
a_1	0.082	0.065	1.252	0.142
a_2	-0.011	0.055	-0.204	-0.023
SD	-0.135	0.063	-2.162*	-0.233
Intercept	0.997	0.067	14.960***	NA
d) Mean of simulated densities (Adj. $R^2 = -0.0001$; $F_{3,81} = 0.996$)				
a_1	0.046	0.078	0.595	0.069
a_2	0.030	0.066	0.461	0.054
SD	0.114	0.749	1.519	0.167
Intercept	0.837	0.08	10.498***	NA

Notes: Results on temporal variance [temporal variance ~ direct density effect (a_1) + delayed density effect (a_2) + density independent effect (SD)] are shown for (a) empirical densities and (b) simulated densities.

Results on temporal mean [temporal mean ~ direct density effect (a_1) + delayed density effect (a_2) + density independent effect (SD)] are given in (c) for empirical densities and in (d) for simulated densities. The model fitting was assessed by adjusted (Adj.) R^2 and F statistics.

* $P < 0.05$, ** $P < 0.01$, *** $P < 0.001$, NA: Not Applicable because the intercept is a constant.

temporal variance (variance over time) of the Bayesian estimated population density was approximately a power law function of the temporal mean (mean over time). This finding illustrated the temporal TL. The slope of the log(variance)–log(mean) relationship was estimated to be $b \pm$ standard error = 1.613 ± 0.141 (Appendix S1: Table S1). The estimated density also satisfied a spatial TL. The slope was estimated to be $b \pm$ standard error = 1.430 ± 0.132 (Appendix S1: Table S2). There was no statistically significant evidence of nonlinearity in temporal or spatial relationships.

Interpretation of the slope of Taylor's law

The slope b of TL is not an indicator of the absolute level of variation in population density. Rather, b is an “elasticity,” in economic jargon, that is, b is approximately the proportional rate of increase of the variance of population density associated with a given proportional increase in the mean of population density. For example, if $b = 1.613$, as in the observed temporal TL, and if a first population has temporal mean density that is 1% larger than that of a second population, so that $\bar{N}_1 = 1.01 \times \bar{N}_2$, then, on average, the first population will have a temporal

variance of population density very nearly (but not exactly) 1.613% larger than that of the second, because

$$\begin{aligned} \text{Var}(N_1) &= a(\bar{N}_1)^{1.613} = a(1.01 \times \bar{N}_2)^{1.613} \\ &= 1.01^{1.613} \times a(\bar{N}_2)^{1.613} \approx 1.01618 \times \text{Var}(N_2). \end{aligned}$$

In general, if ϵ is much smaller than 1 (in the example, $\epsilon = 0.01 \ll 1$, where ϵ is the fractional change in the mean), then $(1 + \epsilon)^b \approx 1 + b \times \epsilon$ so if the mean is increased by the factor $1 + \epsilon$ or by 100%, then the variance is increased approximately by the factor $1 + b \times \epsilon$ or by $100b \times \epsilon\%$. The smaller ϵ is, the more accurate the approximation is.

The coefficient of variation is defined as the standard deviation divided by the mean. When TL has slope $0 < b < 2$, as for these vole populations, a population that is more abundant on average has a larger variance but smaller coefficient of variation.

Simulations of the Gompertz model

Previously, the population dynamics of gray-sided voles at the study sites had been shown to be described well by the Gompertz model (Eq. 2). In this linear autoregressive model, the dynamic variable was the logarithm of population density, and density dependence operated

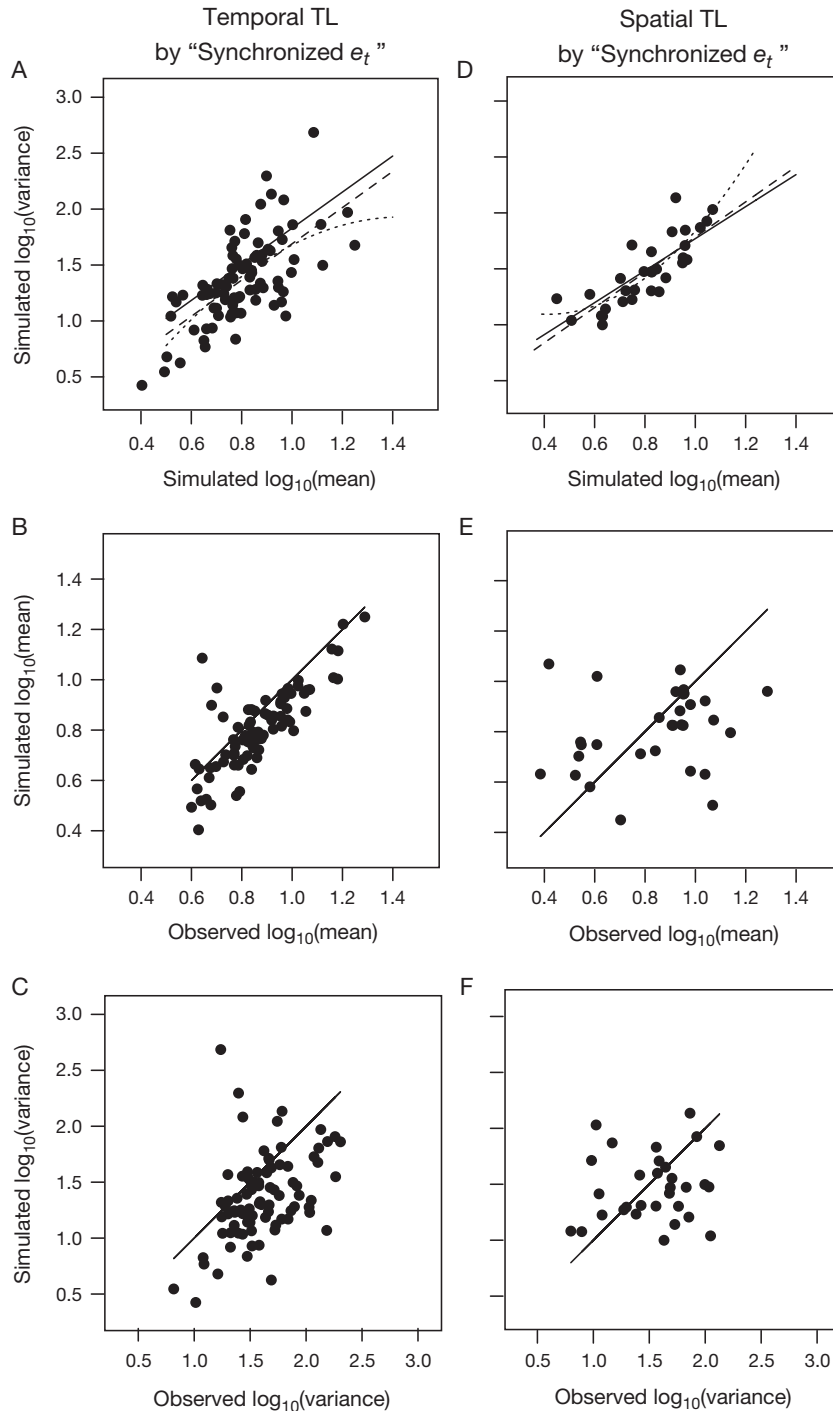


FIG. 3. The temporal (A, B, and C) and spatial (D, E, and F) TLs, means, and variances in 85 Synchronized e_t simulations, each lasting 31 years, which were generated using observed $a_{1,j}$, observed $a_{2,j}$, and synchronized $e_{t,j}$. (A) The $\log_{10}(\text{temporal variance})$ as a function of $\log_{10}(\text{temporal mean})$ for the simulated populations. The solid line is the OLS regression for the observed populations. The broken and dotted lines represent the linear and quadratic relationship in the simulations, respectively. (B) The $\log_{10}(\text{temporal mean})$ of the Synchronized e_t simulations as a function of the $\log_{10}(\text{temporal mean})$ of the observed populations. The solid line represents $y = x$. (C) The relationship of $\log_{10}(\text{temporal variance})$ between the observed populations and the Synchronized e_t simulations. The solid line represents $y = x$. (D) The $\log_{10}(\text{spatial variance})$ as a function of $\log_{10}(\text{spatial mean})$ for the simulated populations. The solid line is the OLS regression for the observed populations. The broken and dotted lines represent the linear and quadratic relationship in the simulations, respectively. (E) The relationship of $\log_{10}(\text{spatial mean})$ between the observed populations and the Synchronized e_t simulations. The solid line represents $y = x$. (F) The relationship of $\log_{10}(\text{spatial variance})$ between the observed populations and the Synchronized e_t simulations. The solid line represents $y = x$.

with 1-yr lags (quantified by parameter a_1) and 2-yr lags (quantified by parameter a_2). Density-independent random effects (quantified by parameter SD) were assumed independent in time and space but with standard deviations that varied from site to site.

The GLM model including all parameters of the Gompertz model (a_1 , a_2 , and SD) had significant ability to explain the variation of the variance of densities, but not variation in the mean of densities (Table 1). Since the estimated mean of an observed population was given as an equilibrium density to simulations, the mean of simulated densities was very probably influenced more by the estimated mean than by the three parameters of the Gompertz model. The parameters may have indirectly influenced the mean of simulated densities through influencing the variability of densities.

To investigate whether the Gompertz model could account for the observed temporal and spatial TLs, we performed three sets of simulations under differing assumptions. In all sets of simulations, $\log(\text{temporal variance})$ was approximately a linear function of $\log(\text{temporal mean})$, and $\log(\text{spatial variance})$ was approximately a linear function of $\log(\text{spatial mean})$, confirming that the Gompertz model could generate the *form* of a temporal and a spatial TL.

However, the temporal and spatial TLs in the Fundamental simulation were significantly steeper than the observed temporal and spatial TLs. The temporal TL slope of the Fundamental simulation (2.699 ± 0.214) was higher than 2. The slopes of TL that are commonly observed in many empirical examples lie between 1 and 2 (Taylor and Woiwod 1980). The slopes of the temporal and spatial TLs of the observed vole populations (1.613 ± 0.141 and 1.430 ± 0.132) were also included in this range.

Modified simulations of the Gompertz model

To make the Gompertz model's TLs have parameters that matched the parameters of the observed TLs, we incorporated two ecological effects, the heterogeneity of habitat quality and the synchrony of density independent factors. These simulations differed from the Fundamental simulations in two respects: the standard deviation of the density-independent error term was reduced by the equation of $\text{Adjusted SD}_j = \text{estimated SD}_j - 0.174 \times \log_e(\text{estimated temporal mean})$ for each j , and the density-independent error term was spatially correlated with correlation $\rho^2 = (0.617)^2 = 0.381$, resulting in an average (over pairs) value of the pairwise correlation between simulated time series of 0.201, not far from the observed average pairwise correlation of 0.297.

In Adjusted SD simulations, we assumed that populations in low-quality habitats have lower mean density but higher variability, whereas populations in high-quality habitats have higher mean density and lower variance of density. This assumption may be realistic. Population densities in low-quality habitats may usually be low but they sometimes become unusually high due to

immigrants from a population in a high-quality habitat in outbreak years. Since differences in densities between usual and outbreak years may be higher in populations in low-quality habitats in comparison with those in high-quality habitats, the negative relationship between temporal mean and SD could realistically be expected.

The Adjusted SD simulations, which realistically approximated the temporal TL, reproduced the form of the spatial TL but implied a slope far larger than that of the observed spatial TL. In the Synchronized e_t simulations, in which the density-independent error terms (e_t) in the Gompertz model were correlated across space (while retaining independence in time), every parameter of the regression of $\log(\text{spatial variance})$ as a function of $\log(\text{spatial mean})$ (in particular, $b \pm \text{standard error} = 1.658 \pm 0.141$, Appendix S1: Table S6) was similar to that for the observed spatial TL. In addition, the Synchronized e_t simulations reproduced the temporal TL (Appendix S1: Table S7), with simulated slope $b \pm \text{standard error} = 1.596 \pm 0.227$. There was no statistically significant evidence of nonlinearity in the Synchronized e_t simulations, nor of a difference in intercept or slope of a temporal TL between the Synchronized e_t simulations and the observed populations.

Interpretation of the modified simulations in terms of ecological mechanisms

We interpreted the effects on the TL slope of the adjustments in the Synchronized e_t simulations in terms of a simple simulation model that assumed some habitats were more favorable for vole population density than others. The details of this simulation are not presented here, as the model served for conceptual exploration rather than quantitative explanation. In this model, habitat heterogeneity was represented by the variation of carrying capacity. Each population grew following the logistic equation and fluctuated with stochastic effects. Movements occurred from a population in a higher quality habitat (a source population) to a neighboring population in a lower quality habitat (a sink population) when the density of the population in the higher quality habitat exceeded its carrying capacity.

Simulations of this model generated the following results. When each population was independent, the spatial and the temporal slopes of TL were higher than 2, and therefore higher than observed. When density-dependent movements were introduced, the spatial and temporal slopes of TL were lowered to the interval between 1 and 2 of the observed spatial and temporal TL slopes.

We understand the effects of the assumptions of this model on the temporal TL as follows. Movements from a population in a higher-quality habitat to a population in a lower-quality habitat when the density of the population in a higher-quality habitat exceeded the carrying capacity reduced the temporal mean and variance of the populations in higher-quality habitats and enhanced the temporal mean and variance of the populations in lower-quality habitats. Since the absolute densities that were subtracted

or added were equal, the relative densities added to the populations in lower-quality habitats were higher than those subtracted from the populations in higher-quality habitats. Thus the assumed population movements would be expected to lower the slope of the temporal TL.

We understand the effects of the assumptions of this model on the spatial TL as follows. Movements from a population in a higher-quality habitat to a population in a lower-quality habitat when the population density in a higher-quality habitat exceeded the carrying capacity reduced the densities of populations in higher-quality habitats and enhanced the densities of populations in lower-quality habitats. Therefore, the spatial variance was reduced by the movements, whereas the spatial mean was not affected by the movement. In a year having higher spatial mean densities, populations in higher-quality habitat were prone to exceed their carrying capacity. As a result, the assumed population movements would be expected to lower the slope of the spatial TL.

This hypothesis has three strengths. First, it explains the milder slopes of the observed temporal and the spatial TL by a single, simple mechanism, namely, density-dependent movement in a source–sink dynamics system. Second, the concept of source–sink dynamics is well established. Demographic surpluses in higher-quality habitats (sources) and deficits in lower-quality habitats (sinks) commonly arise, and movement among local populations can stabilize dynamics at regional scales (Dias 1996, Heinrichs et al. 2016). Third, there is some evidence of density-dependent dispersal in voles, although this topic is controversial (Berthier et al. 2006).

Future research questions

We are not aware of mathematics that shows analytically that the Gompertz model with or without adjustments can generate temporal and spatial TLs, and we are not aware of explicit formulas that express the slopes and intercepts of the temporal and spatial TLs as explicit functions of the parameters of the correlated Gompertz model (a_1 , a_2 , SD , and ρ). Mathematical (by contrast with numerical) analysis of the relation between the Gompertz model, Eq. 2, and Taylor's law, Eq. 1, remains an open problem.

Since the Synchronized e_t simulation showed good agreement with the observed TLs, we suggested that the heterogeneity of habitat quality and the synchrony of some density-independent factor lowered the spatial and temporal TL slope. This statement should be regarded as a hypothesis about nature for further empirical testing and mathematical analysis.

The success of the Synchronized e_t simulations indicated that density dependence may be a driving force leading to the TLs. Since density dependence is the necessary and sufficient condition for sustainable populations (Royama 1992) and density dependence prevails in real populations (Brook and Bradshaw 2006), we suggest one possible answer to the question about why TL is so

widely observed: sustainable populations may have a kind of density dependence that brings about TL. This suggested answer leads to further questions: why and how does some kind of density dependence form TLs, and what kinds of density dependence lead to TL?

The log(spatial mean) and log(spatial variance) of density did not agree well between the Synchronized e_t simulations and the observed populations (Fig. 3E and F), even though the spatial TL, Fig. 3D (as well as the temporal TL, Fig. 3A) generated by the Synchronized e_t simulations did agree well with the corresponding TLs of the data. Each data point in Fig. 3E and F is an average or a variance over 85 populations in 1 yr. While we could estimate the magnitude of stochastic effects on each population's entire dynamics for the study period as SD, we could not predict or model temporal changes in stochastic effects (for example, why some years were peaks and some years were troughs). Therefore, the sequence of the degree of stochastic effects used in the simulations did not fit that for observed populations, and the spatial mean and variance of simulated populations differed from the observed ones. In future work, it would be of interest to examine whether meteorological or other environmental factors like sea surface temperature may play a causal role in the fluctuations of population density that we now treat as stochastic variability.

This study illustrates a scientific application of Taylor's laws that may be useful elsewhere, namely, using TLs as additional criteria to evaluate population-dynamic models. In this study, the previously verified Gompertz model could not reproduce quantitatively the empirically estimated slopes of the TLs. Taking account of habitat quality and synchrony accounted quantitatively for the slopes of observed TLs. In other cases where TLs are verified, testing whether population-dynamic models can account for them may lead to improved assumptions that help link Taylor's law to population dynamics.

ACKNOWLEDGMENTS

T. Saitoh thanks the Forestry Agency of Japanese Government for providing the data. Keiichi Fukaya and Hayato Iijima gave T. Saitoh helpful advice for statistical analyses. J. E. Cohen thanks Priscilla K. Rogerson for assistance and U.S. National Science Foundation grant DMS-1225529 for partial support.

LITERATURE CITED

- Andreassen, H. P., P. Glorvigen, A. Rémy, and R. A. Ims. 2013. New views on how population-intrinsic and community-extrinsic processes interact during the vole population cycles. *Oikos* 122:507–515.
- Bechinski, E. J., and L. P. Pedigo. 1981. Population dispersion and development of sampling plans for *Orius insidiosus* and *Nabis* spp. in soybeans. *Environmental Entomology* 10:956–959.
- Berthier, K., N. Charbonnel, M. Galan, Y. Chaval, and J. F. Cosson. 2006. Migration and recovery of the genetic diversity during the increasing density phase in cyclic vole populations. *Molecular Ecology* 15:2665–2676.

- Brook, B. W., and C. J. A. Bradshaw. 2006. Strength of evidence for density dependence in abundance time series of 1198 species. *Ecology* 87:1445–1451.
- Cohen, J. E., M. Xu, and W. S. F. Schuster. 2013. Stochastic multiplicative population growth predicts and interprets Taylor's power law of fluctuation scaling. *Proceedings of the Royal Society B* 280:20122955.
- Csilléry, K., O. François, and M. G. B. Blum. 2012. abc: an R package for approximate Bayesian computation (ABC). *Methods in Ecology and Evolution* 3:475–479.
- Dias, P. C. 1996. Sources and sinks in population biology. *Trends in Ecology and Evolution* 11:326–330.
- Eisler, Z., I. Bartos, and J. Kertész. 2008. Fluctuation scaling in complex systems: Taylor's law and beyond. *Advances in Physics* 57:89–142.
- Heinrichs, J. A., J. J. Lawler, and N. H. Schumaker. 2016. Intrinsic and extrinsic drivers of source-sink dynamics. *Ecology and Evolution* 6:892–904.
- John, A. 2014. Rodent outbreaks and rice pre-harvest losses in Southeast Asia. *Food Security* 6:249–260.
- Kaneko, Y., K. Nakata, T. Saitoh, N. C. Stenseth, and O. N. Bjørnstad. 1998. The biology of the vole *Clethrionomys rufocanus*: a review. *Researches on Population Ecology* 40: 21–37.
- Kogan, M., W. G. Ruesink, and K. McDowell. 1974. Spatial and temporal distribution patterns of the bean leaf beetle, *Cerotoma trifurcata* (Forster), on soybeans in Illinois. *Environmental Entomology* 3:607–617.
- Lai, J., B. Yang, D. Lin, A. J. Kerkhoff, and K. Ma. 2013. The allometry of coarse root biomass: Log-transformed linear regression or nonlinear regression? *PLoS ONE* 8:e77007.
- MathWorks. 2015. MATLAB R2015a. Mathworks, Natick, Massachusetts, USA.
- Packard, G. C. 2009. On the use of logarithmic transformations in allometric analyses. *Journal of Theoretical Biology* 257:515–518.
- Packard, G. C., G. F. Birchard, and T. J. Boardman. 2011. Fitting statistical models in bivariate allometry. *Biological Reviews* 86:549–563.
- Pertoldi, C., S. Faurby, D. H. Reed, J. Knape, M. Björklund, P. Lundberg, V. Kaitala, V. Loeschke, and L. A. Bach. 2014. Scaling of the mean and variance of population dynamics under fluctuating regimes. *Theory in Biosciences* 133:165–173.
- Royama, T. 1992. Analytical population dynamics. Chapman and Hall, London, UK.
- Saitoh, T., N. C. Stenseth, and O. N. Bjørnstad. 1997. Density dependence in fluctuating grey-sided vole populations. *Journal of Animal Ecology* 66:14–24.
- Saitoh, T., N. C. Stenseth, and O. N. Bjørnstad. 1998. Population dynamics of the vole *Clethrionomys rufocanus* in Hokkaido, Japan. *Researches on Population Ecology* 40:61–76.
- Spiegelhalter, D. J., A. Thomas, N. G. Best, and D. Lunn. 2003. WinBUGS user manual (version 1.4). MRC Biostatistics Unit, Institute of Public Health, Cambridge, UK.
- Stenseth, N. C., O. N. Bjørnstad, and T. Saitoh. 1996. A gradient from stable to cyclic populations of *Clethrionomys rufocanus* in Hokkaido, Japan. *Proceedings of the Royal Society B* 263:1117–1126.
- Stenseth, N. C., O. N. Bjørnstad, and T. Saitoh. 1998. Seasonal forcing on the dynamics of *Clethrionomys rufocanus*: modeling geographic gradients in population dynamics. *Researches on Population Ecology* 40:85–95.
- Stenseth, N. C., H. Viljugrein, T. Saitoh, T. F. Hansen, M. O. Kittilsen, E. Bølviken, and F. Glöckner. 2003. Seasonality, density dependence, and population cycles in Hokkaido voles. *Proceedings of the National Academy of Sciences USA* 100:11478–11483.
- Taylor, L. R. 1961. Aggregation, variance and the mean. *Nature* 189:732–735.
- Taylor, L. R. 1986. Synoptic dynamics, migration and the Rothamsted insect survey: Presidential Address to the British Ecological Society, December 1984. *Journal of Animal Ecology* 55:1–38.
- Taylor, L. R., and I. P. Woiwod. 1980. Temporal stability as a density dependent species characteristic. *Journal of Animal Ecology* 49:209–224.
- Taylor, L. R., I. P. Woiwod, and J. N. Perry. 1978. The density-dependence of spatial behaviour and the rarity of randomness. *Journal of Animal Ecology* 47:383–406.
- Tokeshi, M. 1995. On the mathematical basis of the variance-mean power relationship. *Researches on Population Ecology* 37:43–48.
- Wilson, L. T., W. L. Sterling, D. R. Rummel, and J. E. DeVay. 1989. Quantitative sampling principles in cotton. Pages 85–119 in R. E. Frisbie, K. M. El-Zik, and L. T. Wilson, editors. *Integrated pest management systems and cotton production*. John Wiley & Sons, New York, New York, USA.
- Xiao, X., E. P. White, M. B. Hooten, and S. L. Durham. 2011. On the use of log-transformation vs. nonlinear regression for analyzing biological power laws. *Ecology* 92:1887–1894.

SUPPORTING INFORMATION

Additional supporting information may be found in the online version of this article at <http://onlinelibrary.wiley.com/doi/10.1002/cey.1575/supinfo>

20 Running head: Taylor's law in Hokkaido voles

21 Title: Population dynamics, synchrony, and environmental quality of Hokkaido voles lead to
22 temporal and spatial Taylor's laws

23 Authors: Joel E. Cohen¹, Takashi Saitoh²

24 Affiliations:

25 ¹ Laboratory of Populations, The Rockefeller University and Columbia University, 1230 York
26 Ave., Box 20, New York, NY 10065-6399, USA; also Department of Statistics, Columbia
27 University, and Department of Statistics, University of Chicago

28 ² Field Science Center, Hokkaido University, North-11, West-10, Sapporo 060-0811, Japan

29

30 * Corresponding author:

31 Joel E. Cohen

32 Laboratory of Populations, The Rockefeller University and Columbia University, 1230 York
33 Ave., Box 20, New York, NY 10065-6399, USA

34 Email cohen@rockefeller.edu,

Field Cod

35 **SUPPLEMENTARY MATERIAL**

36 *Supplementary Figures S1-S2*

37 *Supplementary Tables S1-S12*

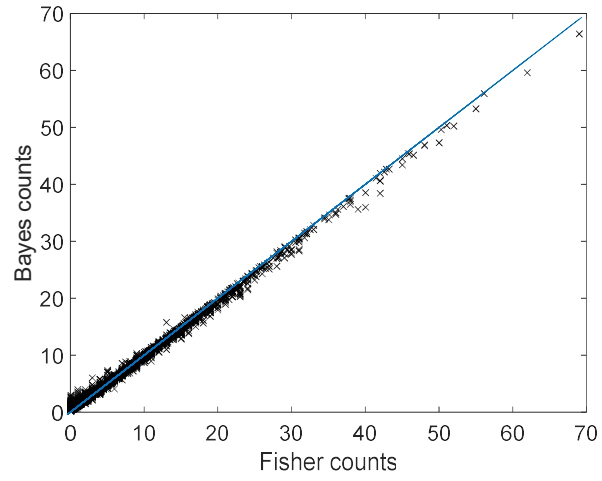
38

39 *Supplementary figures*

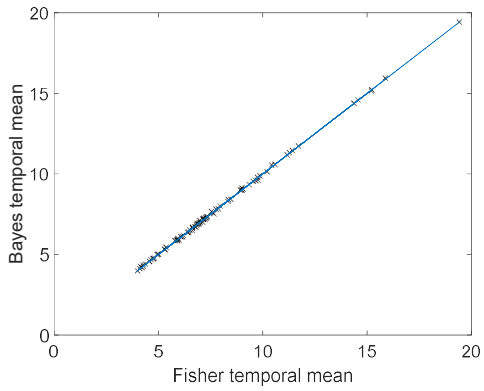
40 Figure S1. Comparison of population density estimates between the frequentist (or "Fisher
41 counts") estimates ($150 \times \text{counts} / \text{sampling effort in trap nights}$) and the Bayesian (or "Bayes
42 counts") estimates by WinBUGS. The solid line represents equality of ordinate and abscissa.
43 (aA) "Bayes counts" against "Fisher counts". (bB) The temporal mean of Bayes counts against
44 the temporal mean of Fisher counts. (cC) The spatial mean of Bayes counts against the spatial
45 mean of Fisher counts. (dD) The temporal variance of Bayes counts against the temporal
46 variance of Fisher counts. (eE) The spatial variance of Bayes counts against the spatial variance
47 of Fisher counts.

48

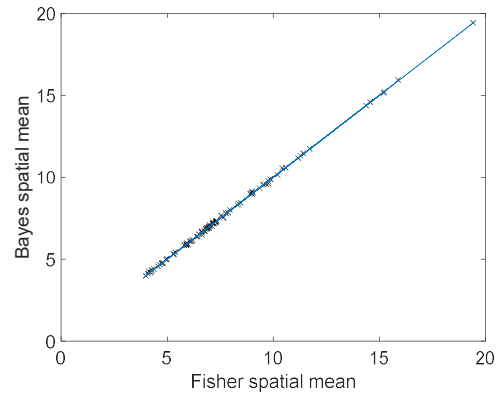
(aA)



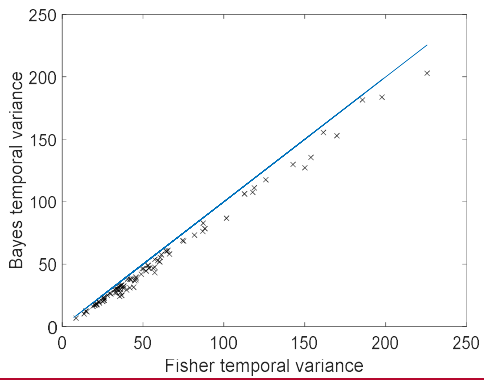
(bB)



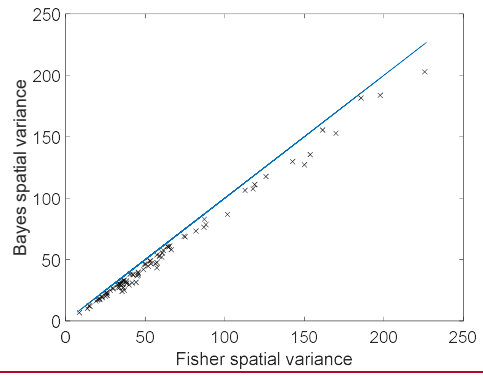
(eC)



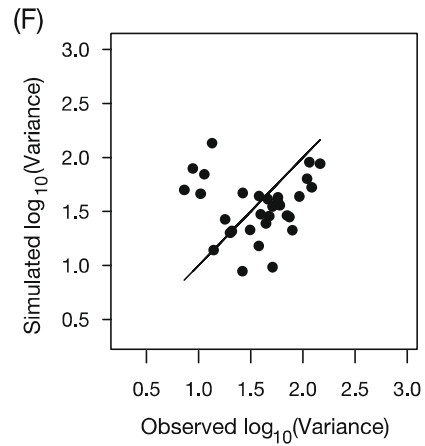
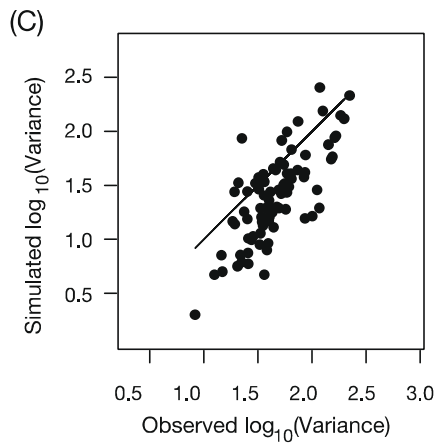
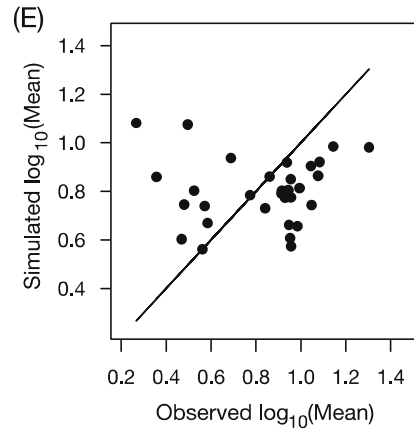
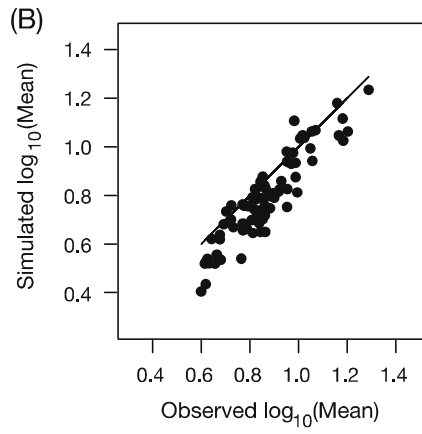
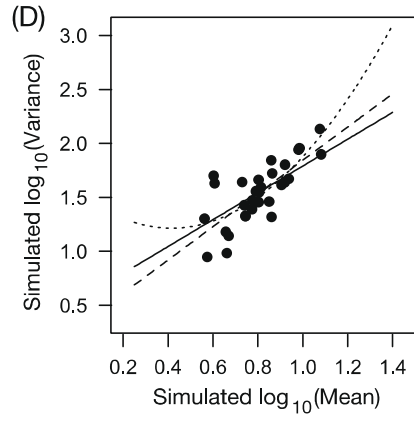
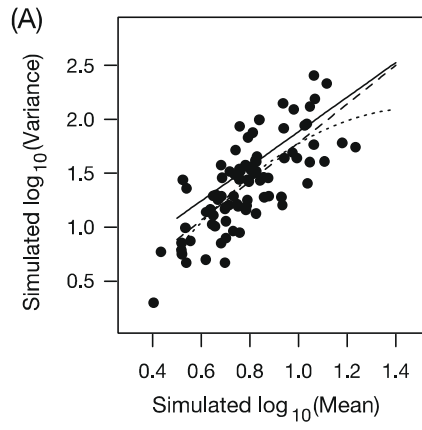
(D)



(E)



51 Figure S2. The temporal (A, B, and C) and spatial (D, E, and F) means, variances and TLs in 85
52 Synchronized e_t simulations, each lasting 31 years, which were generated using observed $a_{1,j}$,
53 observed $a_{2,j}$, and SD_j estimated by the Yule-Walker method and synchronized $e_{t,i}$ (see Tables S8
54 and S9). (A) The \log_{10} (temporal variance) as a function of \log_{10} (temporal mean) for the
55 simulated populations. In (A) and (D), the solid line is the OLS regression for the observed
56 populations, and the broken and dotted lines represent the linear and quadratic relationship in the
57 simulations, respectively. (B) The \log_{10} (temporal mean) of the Synchronized e_t simulations as a
58 function of the \log_{10} (temporal mean) of the observed populations. In (B), (C), (E), and (F), the
59 solid line represents $y = x$. (C) The \log_{10} (temporal variance) of the Synchronized e_t simulations
60 as a function of the \log_{10} (temporal variance) of the observed populations. (D) The \log_{10} (spatial
61 variance) as a function of \log_{10} (spatial mean) of the simulated populations. (E) The relationship
62 of \log_{10} (spatial mean) between the observed populations and the Synchronized e_t simulations. (F)
63 The relationship of \log_{10} (spatial variance) between the observed populations and the
64 Synchronized e_t simulations.



66 **Supplementary tables**

67 Table S1. Summary of analyses of the observed relationship between the sample temporal mean
 68 of population densities [$\log_{10}(\text{temporal mean})$] and the sample temporal variance [$\log_{10}(\text{temporal}$
 69 variance)] over 31 years based on the Bayesian estimates for 85 populations using the linear and
 70 quadratic models.

71 Linear model (Taylor's law): $\text{lm}(\text{formula} = \log_{10}(\text{temporal variance}) \sim \log_{10}(\text{temporal mean}))$

72 Coefficients:	Estimate	SE	95%CI	<i>t</i> -statistic	<i>P</i> value
73 (Intercept)	0.216	0.124	-0.030 – 0.462	1.748	0.084
74 $\log_{10}(\text{temporal mean})$	1.613	0.141	1.332 – 1.894	11.422	<2e-16

75 Residual standard error: 0.191 on 83 degrees of freedom

76 Multiple R^2 : 0.611, Adjusted R^2 : 0.607

77 *F*-statistic: 130.5 on 1 and 83 DF, *P* value: < 2.2e-16

78 -----

79 Quadratic model: $\text{lm}(\text{formula} = \log_{10}(\text{temporal variance}) \sim \text{I}(\log_{10}(\text{temporal mean})^2) +$
 80 $\log_{10}(\text{temporal mean}))$

81 Coefficients:	Estimate	SE	95%CI	<i>t</i> -statistic	<i>P</i> value
82 (Intercept)	-0.477	0.562	-1.595 – 0.641	-0.849	0.398
83 $\log_{10}(\text{temporal mean})^2$	-0.879	0.695	-2.263 – 0.504	-1.265	0.210
84 $\log_{10}(\text{temporal mean})$	3.197	1.261	0.689 – 5.705	2.536	0.013

85 Residual standard error: 0.19 on 82 degrees of freedom

86 Multiple R^2 : 0.619, Adjusted R^2 : 0.609

87 *F*-statistic: 66.5 on 2 and 82 DF, *P* value: < 2.2e-16

88 Table S2. Summary of analyses of the observed relationship between the sample spatial mean of
 89 population densities [$\log_{10}(\text{spatial mean})$] and the sample spatial variance [$\log_{10}(\text{spatial}$
 90 variance)] over the 85 populations based on the Bayesian estimates for 31 years using the linear
 91 and quadratic models.

92

93 Linear model (Taylor's law): $\text{lm}(\text{formula} = \log_{10}(\text{spatial variance}) \sim \log_{10}(\text{spatial mean}))$

94 Coefficients:	Estimate	SE	95%CI	<i>t</i> -statistic	<i>P</i> value
95 (Intercept)	0.339	0.114	0.106 – 0.575	2.969	0.006
96 $\log_{10}(\text{spatial mean})$	1.430	0.132	1.160 – 1.700	10.831	1.05e-11

97

98 Residual standard error: 0.165 on 29 degrees of freedom

99 Multiple R^2 : 0.802, Adjusted R^2 : 0.795

100 *F*-statistic: 117.3 on 1 and 29 DF, *P* value: 1.047e-11

101 -----

102 Quadratic model: $\text{lm}(\text{formula} = \log_{10}(\text{spatial variance}) \sim \text{I}(\log_{10}(\text{spatial mean})^2) + \log_{10}(\text{spatial}$
 103 mean))

104 Coefficients:	Estimate	SE	95%CI	<i>t</i> -statistic	<i>P</i> value
105 (Intercept)	0.326	0.352	-0.394 – 1.047	0.928	0.361
106 $\log_{10}(\text{spatial mean})^2$	-0.022	0.576	-1.203 – 1.158	-0.039	0.969
107 $\log_{10}(\text{spatial mean})$	1.466	0.923	-0.426 – 3.358	1.588	0.124

108 Residual standard error: 0.168 on 28 degrees of freedom

109 Multiple R^2 : 0.802, Adjusted R^2 : 0.788

110 F -statistic: 56.64 on 2 and 28 DF, P value: 1.44e-10

111 Table S3. Summary of analyses of the relationship between \log_{10} (temporal mean) of density and
 112 \log_{10} (temporal variance) of density over 31 years for the 85 populations in the Fundamental
 113 simulation based on the Bayesian estimates. Linear and quadratic models were fitted, and an
 114 analysis of covariance used “observed” or “simulated” as covariate.

115

116 Linear model (Taylor's law): $\text{lm}(\text{formula} = \log_{10}(\text{temporal variance}) \sim \log_{10}(\text{temporal mean}))$

117 Coefficients:	Estimate	SE	95%CI	<i>t</i> -statistic	<i>P</i> value
118 (Intercept)	-0.556	0.208	-0.970 – -0.143	-2.676	0.009
119 \log_{10} (temporal mean)	2.699	0.214	2.273 – 3.126	12.592	< 2.2e-16

120 Residual standard error: 0.340 on 83 degrees of freedom

121 Multiple R^2 : 0.656, Adjusted R^2 : 0.652

122 *F*-statistic: 158.6 on 1 and 83 DF, *P* value: < 2.2e-16

123 -----

124 Quadratic model: $\text{lm}(\text{formula} = \log_{10}(\text{temporal variance}) \sim \text{I}(\log_{10}(\text{temporal mean})^2) +$
 125 $\log_{10}(\text{temporal mean}))$

126 Coefficients:	Estimate	SE	95%CI	<i>t</i> -statistic	<i>P</i> value
127 (Intercept)	0.322	0.968	-1.603 – 2.248	0.333	0.740
128 $\log_{10}(\text{temporal mean})^2$	0.910	0.979	-1.038 – 2.858	0.929	0.356
129 $\log_{10}(\text{temporal mean})$	0.882	1.967	-3.031 – 4.795	0.449	0.655

130 Residual standard error: 0.340 on 82 degrees of freedom

131 Multiple R^2 : 0.660, Adjusted R^2 : 0.652

132 *F*-statistic: 79.58 on 2 and 82 DF, *P* value: < 2.2e-16

133 -----

134 Analysis of covariance: simulated \log_{10} (temporal variance) and observed \log_{10} (temporal
135 variance) as a single vector as a linear function of simulated \log_{10} (temporal mean) and observed
136 \log_{10} (temporal mean) as a single vector, observed/simulated indicator (o/s), and their interaction

137 Model: $\text{lm}(\text{formula} = \log_{10}(\text{temporal variance}) \sim \log_{10}(\text{temporal mean}) * \text{o/s})$

138	Coefficients:	Estimate	SE	95%CI	<i>t</i> -statistic	<i>P</i> value
139	(Intercept)	0.216	0.179	-0.136 – 0.569	1.210	0.228
140	\log_{10} (temporal mean)	1.613	0.204	1.210 – 2.016	7.910	3.44e-13
141	o/s	-0.772	0.246	-1.257 – -0.288	-3.145	0.002
142	\log_{10} (temporal mean): o/s	1.086	0.268	0.557 – 1.615	4.054	7.72e-5

143 Residual standard error: 0.275 on 166 degrees of freedom

144 Multiple R^2 : 0.706, Adjusted R^2 : 0.701

145 *F*-statistic: 132.8 on 3 and 166 DF, *P* value: < 2.2e-16

146 -----

147 Simulated \log_{10} (temporal mean) as a linear function of observed \log_{10} (temporal mean)

148 Model: $\text{lm}(\text{formula} = \text{Simulated } \log_{10}(\text{temporal mean}) \sim \text{observed } \log_{10}(\text{temporal mean}))$

149	Coefficients:	Estimate	SE	95%CI	<i>t</i> -statistic	<i>P</i> value
150	(Intercept)	0.465	0.097	0.243 – 0.628	4.499	2.2e-5
151	observed \log_{10} (temporal mean)	0.601	0.111	0.381 – 0.821	5.438	5.31e-7

152 Residual standard error: 0.149 on 83 degrees of freedom

153 Multiple R^2 : 0.263, Adjusted R^2 : 0.254

154 *F*-statistic: 29.58 on 1 and 83 DF, *P* value: 5.31e-7

155 -----

156 Simulated \log_{10} (temporal variance) as a linear function of observed \log_{10} (temporal variance)

157 Model: $\text{lm}(\text{formula} = \text{Simulated } \log_{10}(\text{temporal variance}) \sim \text{observed } \log_{10}(\text{temporal variance}))$

158	Coefficients:	Estimate	SE	95%CI	<i>t</i> -statistic	<i>P</i> value
159	(Intercept)	0.787	0.311	0.169 – 1.406	2.531	0.013
160	observed \log_{10} (temporal variance)	0.766	0.190	0.388 – 1.144	4.031	0.0001

161 Residual standard error: 0.530 on 83 degrees of freedom

162 Multiple R^2 : 0.164, Adjusted R^2 : 0.154

163 *F*-statistic: 16.25 on 1 and 83 DF, *P* value: 0.0001

164

165 Table S4. Summary of analyses of the relationship between \log_{10} (temporal mean) of density and
 166 \log_{10} (temporal variance) of density over 31 years for the 85 populations in the Adjusted SD
 167 simulations based on the Bayesian estimates, where adjusted standard deviation of the density-
 168 independent term = $SD_j - 0.174 \times \log_e(\text{estimated temporal mean})$ for each j ; SD_j is the standard
 169 deviation of density-independent perturbations estimated from data of population j . Linear and
 170 quadratic models were fitted, and an analysis of covariance used “observed” or “simulated” as
 171 covariate.

172

173 Linear model (Taylor's law): $\text{lm}(\text{formula} = \log_{10}(\text{temporal variance}) \sim \log_{10}(\text{temporal mean}))$

174 Coefficients:	Estimate	SE	95%CI	<i>t</i> -statistic	<i>P</i> value
175 (Intercept)	0.079	0.274	-0.466 – 0.624	0.289	0.774
176 \log_{10} (temporal mean)	1.671	0.321	1.032 – 2.310	5.199	1.41e-6

177 Residual standard error: 0.437 on 83 degrees of freedom

178 Multiple R^2 : 0.246, Adjusted R^2 : 0.237

179 *F*-statistic: 27.03 on 1 and 83 DF, *P* value: 1.41e-6

180 -----

181 Quadratic model: $\text{lm}(\text{formula} = \log_{10}(\text{temporal variance}) \sim \text{I}(\log_{10}(\text{temporal mean})^2) +$
 182 $\log_{10}(\text{temporal mean}))$

183

184 Coefficients:	Estimate	SE	95%CI	<i>t</i> -statistic	<i>P</i> value
185 (Intercept)	-0.512	1.279	-3.057 – 2.033	-0.401	0.690
186 $\log_{10}(\text{temporal mean})^2$	-0.837	1.768	-4.355 – 2.681	-0.473	0.637
187 $\log_{10}(\text{temporal mean})$	3.100	3.036	-2.939 – 9.139	1.021	0.310

188 Residual standard error: 0.467 on 82 degrees of freedom

189 Multiple R^2 : 0.247, Adjusted R^2 : 0.229

190 F -statistic: 13.5 on 2 and 82 DF, P value: 8.55e-6

191 -----

192 Analysis of covariance: simulated \log_{10} (temporal variance) and observed \log_{10} (temporal
193 variance) as a single vector as a linear function of simulated \log_{10} (temporal mean) and observed
194 \log_{10} (temporal mean) as a single vector, observed/simulated indicator (o/s), and their interaction

195 Model: $\text{lm}(\text{formula} = \log_{10}(\text{temporal variance}) \sim \log_{10}(\text{temporal mean}) * \text{o/s})$

196	Coefficients:	Estimate	SE	95%CI	t -statistic	P value
197	(Intercept)	0.216	0.228	-0.215 – 0.647	0.990	0.324
198	\log_{10} (temporal mean)	1.613	0.249	1.120 – 2.105	6.467	1.07e-9
199	o/s	-0.137	0.304	-0.737 – 0.463	-0.451	0.653
200	\log_{10} (temporal mean):o/s	0.058	0.352	-0.636 – 0.753	0.165	0.869

201 Residual standard error: 0.337 on 166 degrees of freedom

202 Multiple R^2 : 0.360, Adjusted R^2 : 0.348

203 F -statistic: 31.06 on 3 and 166 DF, P value: 5.44e-16

204 -----

205 Simulated \log_{10} (temporal mean) as a linear function of observed \log_{10} (temporal mean)

206 Model: $\text{lm}(\text{formula} = \text{Simulated } \log_{10}(\text{temporal mean}) \sim \text{observed } \log_{10}(\text{temporal mean}))$

207	Coefficients:	Estimate	SE	95%CI	t -statistic	P value
208	(Intercept)	0.189	0.064	0.061 – 0.316	2.950	0.004

209 observed \log_{10} (temporal mean) 0.754 0.073 0.609 – 0.899 10.33 <2e-16

210 Residual standard error: 0.099 on 83 degrees of freedom

211 Multiple R^2 : 0.562, Adjusted R^2 : 0.557

212 F-statistic: 106.7 on 1 and 83 DF, p-value: < 2.2e-16

213 -----

214 Simulated \log_{10} (temporal variance) as a linear function of observed \log_{10} (temporal variance)

215 Model: $\text{lm}(\text{formula} = \text{Simulated } \log_{10}(\text{temporal variance}) \sim \text{observed } \log_{10}(\text{temporal variance}))$

216	Coefficients:	Estimate	SE	95%CI	t-statistic	P value
217	(Intercept)	0.364	0.268	-0.168 – 0.896	1.360	0.177
218	observed \log_{10} (temporal variance)	0.695	0.164	0.370 – 1.020	4.253	5.49e-05

219 Residual standard error: 0.455 on 83 degrees of freedom

220 Multiple R^2 : 0.179, Adjusted R^2 : 0.169

221 F-statistic: 18.09 on 1 and 83 DF, P value: 5.49e-05

222

223 Table S5. Summary of analyses of the relationship between $\log_{10}(\text{spatial mean})$ of density and
 224 $\log_{10}(\text{spatial variance})$ over the 85 populations for 31 years in the Adjusted SD simulations based
 225 on the Bayesian estimates, where adjusted standard deviation of the density-independent term =
 226 $SD_j - 0.174 \times \log_e(\text{estimated temporal mean})$ for each j ; SD_j is the standard deviation of error
 227 estimated from data of population j . Linear and quadratic models were fitted, and an analysis of
 228 covariance used “observed” or “simulated” as covariate.

229

230 Linear model (Taylor's law): $\text{lm}(\text{formula} = \log_{10}(\text{spatial variance}) \sim \log_{10}(\text{spatial mean}))$

231	Coefficients:	Estimate	SE	95%CI	<i>t</i> -statistic	<i>P</i> value
232	(Intercept)	-1.094	0.400	-1.912 – -0.275	-2.733	0.011
233	$\log_{10}(\text{spatial mean})$	3.283	0.464	2.334 – 4.233	7.073	8.83e-08

234 Residual standard error: 0.199 on 29 degrees of freedom

235 Multiple R^2 : 0.633, Adjusted R^2 : 0.620

236 *F*-statistic: 50.02 on 1 and 29 DF, *P* value: 8.83e-08

237 -----

238 Quadratic model: $\text{lm}(\text{formula} = \log_{10}(\text{spatial variance}) \sim \text{I}(\log_{10}(\text{spatial mean})^2) + \log_{10}(\text{spatial mean}))$
 239 mean))

240	Coefficients:	Estimate	SE	95%CI	<i>t</i> -statistic	<i>P</i> value
241	(Intercept)	5.802	1.679	2.362 – 9.242	3.455	0.002
242	$\log_{10}(\text{spatial mean})^2$	10.703	2.559	5.461 – 15.944	4.183	0.0002
243	$\log_{10}(\text{spatial mean})$	-14.011	4.151	-22.514 – -5.508	-3.375	0.002

244 Residual standard error: 0.158 on 28 degrees of freedom

245 Multiple R^2 : 0.774, Adjusted R^2 : 0.758

246 *F*-statistic: 47.99 on 2 and 28 DF, *P* value: 8.98e-10

247 -----

248 Analysis of covariance: simulated $\log_{10}(\text{spatial variance})$ and observed $\log_{10}(\text{spatial variance})$ as
249 a single vector as a linear function of simulated $\log_{10}(\text{spatial mean})$ and observed $\log_{10}(\text{spatial}$
250 mean) as a single vector, observed/simulated indicator (o/s), and their interaction

251 Model: $\text{lm}(\text{formula} = \log_{10}(\text{spatial variance}) \sim \log_{10}(\text{spatial mean}) * \text{o/s})$

252	Coefficients:	Estimate	SE	95%CI	<i>t</i> -statistic	<i>P</i> value
253	(Intercept)	0.339	0.127	0.086 – 0.593	2.268	0.001
254	$\log_{10}(\text{spatial mean})$	1.430	0.146	1.138 – 1.723	9.784	6.93e-14
255	o/s	-1.433	0.389	-2.212 – -0.655	-3.684	0.001
256	$\log_{10}(\text{spatial mean}): \text{o/s}$	1.853	0.451	0.950 – 2.756	4.109	0.0001

257 Residual standard error: 0.183 on 58 degrees of freedom

258 Multiple R^2 : 0.748, Adjusted R^2 : 0.735

259 *F*-statistic: 57.28 on 3 and 58 DF, *P* value: 2.2e-16

260 -----

261 Simulated $\log_{10}(\text{spatial mean})$ as a linear function of observed $\log_{10}(\text{spatial mean})$

262 Model: $\text{lm}(\text{formula} = \text{simulated } \log_{10}(\text{spatial mean}) \sim \text{observed } \log_{10}(\text{spatial mean}))$

263	Coefficients:	Estimate	SE	95%CI	<i>t</i> -statistic	<i>P</i> value
264	(Intercept)	0.808	0.054	0.697 – 0.918	14.902	3.98e-15
265	observed $\log_{10}(\text{spatial mean})$	0.061	0.063	-0.067 – 0.189	0.977	0.337

266 Residual standard error: 0.078 on 29 degrees of freedom

267 Multiple R^2 : 0.032, Adjusted R^2 : -0.001

268 F -statistic: 0.954 on 1 and 29 DF, P value: 0.337

269 -----

270 Simulated $\log_{10}(\text{spatial variance})$ as a linear function of observed $\log_{10}(\text{spatial variance})$

271 Model: $\text{lm}(\text{formula} = \text{simulated } \log_{10}(\text{spatial variance}) \sim \text{observed } \log_{10}(\text{spatial variance}))$

272	Coefficients:	Estimate	SE	95%CI	t -statistic	P value
273	(Intercept)	1.535	0.257	1.011 – 2.060	5.984	1.66e-06
274	observed $\log_{10}(\text{spatial variance})$	0.124	0.163	-0.209 – 0.457	0.761	0.453

275 Residual standard error: 0.325 on 29 degrees of freedom

276 Multiple R^2 : 0.020, Adjusted R^2 : -0.014

277 F -statistic: 0.579 on 1 and 29 DF, P value: 0.453

278

279 Table S6. Summary of analyses of the relationship between $\log_{10}(\text{spatial mean})$ of density and
 280 $\log_{10}(\text{spatial variance})$ over the 85 populations for 31 years in the Synchronized e_t simulations
 281 based on the Bayesian estimates. Linear and quadratic models were fitted, and an analysis of
 282 covariance used “observed” or “simulated” as covariate.

283

284 Linear model (Taylor's law): $\text{lm}(\text{formula} = \log_{10}(\text{spatial variance}) \sim \log_{10}(\text{spatial mean}))$

285	Coefficients:	Estimate	SE	95%CI	<i>t</i> -statistic	<i>P</i> value
286	(Intercept)	0.208	0.167	-0.133 – 0.550	1.247	0.222
287	$\log_{10}(\text{spatial mean})$	1.575	0.204	1.158 – 1.993	7.721	1.63e-08

288 Residual standard error: 0.176 on 29 degrees of freedom

289 Multiple R^2 : 0.673, Adjusted R^2 : 0.661

290 *F*-statistic: 59.6 on 1 and 29 DF, *P* value: 1.63e-08

291 -----

292 Simulated $\log_{10}(\text{spatial variance})$ as a quadratic function of simulated $\log_{10}(\text{spatial mean})$

293 Model: $\text{lm}(\text{formula} = \log_{10}(\text{spatial variance}) \sim \text{I}(\log_{10}(\text{spatial mean})^2) + \log_{10}(\text{spatial mean}))$

294	Coefficients:	Estimate	SE	95%CI	<i>t</i> -statistic	<i>P</i> value
295	(Intercept)	1.466	0.656	0.123 – 2.810	2.236	0.034
296	$\log_{10}(\text{spatial mean})^2$	2.1691	1.097	-0.078 – 4.417	1.977	0.058
297	$\log_{10}(\text{spatial mean})$	-1.798	1.717	-5.316 – 1.719	-1.047	0.304

298 Residual standard error: 0.168 on 28 degrees of freedom

299 Multiple R^2 : 0.713, Adjusted R^2 : 0.692

300 *F*-statistic: 34.75 on 2 and 28 DF, *P* value: 2.60e-08

301 -----

302 Analysis of covariance: simulated $\log_{10}(\text{spatial variance})$ and observed $\log_{10}(\text{spatial variance})$ as
303 a single vector as a linear function of simulated $\log_{10}(\text{spatial mean})$ and observed $\log_{10}(\text{spatial}$
304 mean) as a single vector, observed/simulated indicator (o/s), and their interaction

305 Model: $\text{lm}(\text{formula} = \log_{10}(\text{spatial variance}) \sim \log_{10}(\text{spatial mean}) * \text{o/s})$

306	Coefficients:	Estimate	SE	95%CI	<i>t</i> -statistic	<i>P</i> value
307	(Intercept)	0.339	0.118	0.103 – 0.576	2.8715	0.006
308	$\log_{10}(\text{spatial mean})$	1.430	0.137	1.158 – 1.704	10.473	5.4e-15
309	o/s	-0.131	0.200	-0.532 – 0.270	-0.655	0.515
310	$\log_{10}(\text{spatial mean})\text{:o/s}$	0.145	0.240	-0.336 – 0.626	0.603	0.549

311 Residual standard error: 0.171 on 58 degrees of freedom

312 Multiple R^2 : 0.751, Adjusted R^2 : 0.738

313 *F*-statistic: 58.39 on 3 and 58 DF, *P* value: < 2.2e-16

314 -----

315 Simulated $\log_{10}(\text{spatial mean})$ as a linear function of observed $\log_{10}(\text{spatial mean})$

316 Model: $\text{lm}(\text{formula} = \text{simulated } \log_{10}(\text{spatial mean}) \sim \text{observed } \log_{10}(\text{spatial mean}))$

317	Coefficients:	Estimate	SE	95%CI	<i>t</i> -statistic	<i>P</i> value
318	(Intercept)	0.667	0.108	0.446 – 0.888	6.186	9.57e-07
319	observed $\log_{10}(\text{spatial mean})$	0.1263	0.125	-0.092 – 0.418	1.304	0.202

320 Residual standard error: 0.1756 on 29 degrees of freedom

321 Multiple R^2 : 0.056, Adjusted R^2 : 0.023

322 *F*-statistic: 1.701 on 1 and 29 DF, *P* value: 0.203

323 -----

324 Simulated $\log_{10}(\text{spatial variance})$ as a linear function of observed $\log_{10}(\text{spatial variance})$

325 Model: $\text{lm}(\text{formula} = \text{simulated } \log_{10}(\text{spatial variance}) \sim \text{observed } \log_{10}(\text{spatial variance}))$

326	Coefficients:	Estimate	SE	95%CI	<i>t</i> -statistic	<i>P</i> value
327	(Intercept)	1.289	0.241	0.797 – 1.781	5.361	9.3e-06
328	observed $\log_{10}(\text{spatial variance})$	0.120	0.153	-0.192 – 0.431	-0.787	0.438

329 Residual standard error: 0.304 on 29 degrees of freedom

330 Multiple R^2 : 0.021, Adjusted R^2 : -0.013

331 *F*-statistic: 0.619 on 1 and 29 DF, *P* value: 0.438

332

333 Table S7. Summary of analyses of the relationship between \log_{10} (temporal mean) of density and
 334 \log_{10} (temporal variance) over 31 years for the 85 populations in the Synchronized e_t simulations
 335 based on the Bayesian estimates. Linear and quadratic models were fitted, and an analysis of
 336 covariance used “observed” or “simulated” as covariate.

337

338 Linear model (Taylor's law): $\text{lm}(\text{formula} = \log_{10}(\text{temporal variance}) \sim \log_{10}(\text{temporal mean}))$

339 Coefficients:	Estimate	SE	95%CI	<i>t</i> -statistic	<i>P</i> value
340 (Intercept)	0.070	0.1963	-0.254 – 0.393	0.427	0.670
341 \log_{10} (temporal mean)	1.619	0.199	1.223 – 2.016	8.120	3.75e-12

342 Residual standard error: 0.288 on 83 degrees of freedom

343 Multiple R^2 : 0.447, Adjusted R^2 : 0.436

344 *F*-statistic: 65.93 on 1 and 83 DF, *P* value: 3.75e-12

345 -----

346 Quadratic model: $\text{lm}(\text{formula} = \log_{10}(\text{temporal variance}) \sim \text{I}(\log_{10}(\text{temporal mean})^2) +$
 347 $\log_{10}(\text{temporal mean}))$

348 Coefficients:	Estimate	SE	95%CI	<i>t</i> -statistic	<i>P</i> value
349 (Intercept)	-0.771	0.541	-1.846 – 0.304	-1.425	0.158
350 \log_{10} (temporal mean) ²	-1.304	0.801	-2.897 – 0.289	-1.628	0.107
351 \log_{10} (temporal mean)	3.753	1.325	1.117 – 6.389	2.832	0.006

352 Residual standard error: 0.285 on 82 degrees of freedom

353 Multiple R^2 : 0.460, Adjusted R^2 : 0.447

354 *F*-statistic: 34.95 on 2 and 82 DF, *P* value: 1.05e-11

355 -----

356 Analysis of covariance: simulated \log_{10} (temporal variance) and observed \log_{10} (temporal
357 variance) as a single vector as a linear function of simulated \log_{10} (temporal mean) and observed
358 \log_{10} (temporal mean) as a single vector, observed/simulated (o/s), and their interaction

359 Model: $\text{lm}(\text{formula} = \log_{10}(\text{temporal variance}) \sim \log_{10}(\text{temporal mean}) * \text{o/s})$

360	Coefficients:	Estimate	SE	95%CI	<i>t</i> -statistic	<i>P</i> value
361	(Intercept)	0.216	0.158	-0.097 – 0.529	1.365	0.174
362	\log_{10} (temporal mean)	1.613	0.181	1.256 – 1.970	8.919	8.3e-16
363	o/s	-0.146	0.210	-0.561 – 0.268	-0.698	0.486
364	\log_{10} (temporal mean):o/s	0.007	0.2647	-0.482 – 0.496	0.027	0.979

365 Residual standard error: 0.244 on 166 degrees of freedom

366 Multiple R^2 : 0.562, Adjusted R^2 : 0.554

367 *F*-statistic: 71.00 on 3 and 166 DF, *P* value: < 2.2e-16

368 -----

369 Simulated \log_{10} (temporal mean) as a linear function of observed \log_{10} (temporal mean)

370 Model: $\text{lm}(\text{formula} = \text{Simulated } \log_{10}(\text{temporal mean}) \sim \text{Observed } \log_{10}(\text{temporal mean}))$

371	Coefficients:	Estimate	SE	95%CI	<i>t</i> -statistic	<i>P</i> value
372	(Intercept)	0.074	0.063	-0.052 – 0.200	1.172	0.244
373	observed \log_{10} (temporal mean)	0.841	0.072	0.697 – 0.985	11.622	< 2.2e-16

374 Residual standard error: 0.098 on 83 degrees of freedom

375 Residual R^2 :0.619, Adjusted R^2 :0.615

376 *F*-statistic: 135.1 on 1 and 83 DF, *P* value: < 2.2e-16

377 -----

378 Simulated \log_{10} (temporal variance) as a linear function of observed \log_{10} (temporal variance)

379 Model: $\text{lm}(\text{formula} = \text{Simulated } \log_{10}(\text{temporal variance}) \sim \text{observed } \log_{10}(\text{temporal variance}))$

380	Coefficients:	Estimate	SE	95%CI	<i>t</i> -statistic	<i>P</i> value
381	(Intercept)	0.508	0.205	0.099 – 0.916	2.473	0.015
382	observed \log_{10} (temporal variance)	0.534	0.125	0.284 – 0.783	4.255	5.46e-05

383 Residual standard error: 0.350 on 83 degrees of freedom

384 Multiple R^2 : 0.179, Adjusted R^2 : 0.169

385 *F*-statistic: 18.11 on 1 and 83 DF, *P* value: 5.46e-05

386

387 Table S8. Summary of analyses of the observed relationship between the sample temporal mean
 388 of population densities [$\log_{10}(\text{temporal mean})$] and the sample temporal variance [$\log_{10}(\text{temporal}$
 389 variance)] over 31 years based on Fisher counts for 85 populations using the linear and quadratic
 390 models.

391

392 Linear model (Taylor's law): $\text{lm}(\text{formula} = \log_{10}(\text{temporal variance}) \sim \log_{10}(\text{temporal mean}))$

393 Coefficients:	Estimate	SE	95%CI	<i>t</i> -statistic	<i>P</i> value
394 (Intercept)	0.282	0.110	0.064 – 0.500	2.569	0.012
395 $\log_{10}(\text{temporal mean})$	1.602	0.126	1.352 – 1.851	12.767	< 2.2e-16

396 Residual standard error: 0.170 on 83 degrees of freedom

397 Multiple R^2 : 0.663, Adjusted R^2 : 0.659

398 *F*-statistic: 163 on 1 and 83 DF, *P* value: < 2.2e-16

399 -----

400 Quadratic model: $\text{lm}(\text{formula} = \log_{10}(\text{temporal variance}) \sim \text{I}(\log_{10}(\text{temporal mean})^2) +$
 401 $\log_{10}(\text{temporal mean}))$

402 Coefficients:	Estimate	SE	95%CI	<i>t</i> -statistic	<i>P</i> value
403 (Intercept)	-0.343	0.493	-1.324 – 0.648	-0.695	0.489
404 $\log_{10}(\text{temporal mean})^2$	-0.795	0.612	-2.012 – 0.422	-1.299	0.198
405 $\log_{10}(\text{temporal mean})$	3.032	1.108	0.828 – 5.235	2.737	0.008

406 Residual standard error: 0.169 on 82 degrees of freedom

407 Multiple R^2 : 0.669, Adjusted R^2 : 0.661

408 *F*-statistic: 83.02 on 2 and 82 DF, *P* value: < 2.2e-16

409 Table S9. Summary of analyses of the observed relationship between the sample spatial mean of
 410 population densities [$\log_{10}(\text{spatial mean})$] and the sample spatial variance [$\log_{10}(\text{spatial}$
 411 variance)] over the 85 populations based on Fisher counts for 31 years using the linear and
 412 quadratic models.

413

414 Linear model (Taylor's law): $\text{lm}(\text{formula} = \log_{10}(\text{spatial variance}) \sim \log_{10}(\text{spatial mean}))$

415 Coefficients:	Estimate	SE	95%CI	<i>t</i> -statistic	<i>P</i> value
416 (Intercept)	0.549	0.105	0.335 – 0.763	5.241	1.30e-05
417 $\log_{10}(\text{spatial mean})$	1.242	0.122	0.993 – 1.491	10.215	4.06e-11

418 Residual standard error: 0.169 on 29 degrees of freedom

419 Multiple R^2 : 0.783, Adjusted R^2 : 0.775

420 *F*-statistic: 104.3 on 1 and 29 DF, *P* value: 4.06e-11

421 -----

422 Quadratic model: $\text{lm}(\text{formula} = \log_{10}(\text{spatial variance}) \sim \text{I}(\log_{10}(\text{spatial mean})^2) + \log_{10}(\text{spatial}$
 423 mean))

424 Coefficients:	Estimate	SE	95%CI	<i>t</i> -statistic	<i>P</i> value
425 (Intercept)	0.680	0.262	0.143 – 1.217	2.593	0.015
426 $\log_{10}(\text{spatial mean})^2$	0.257	0.470	-0.706 – 1.220	0.547	0.589
427 $\log_{10}(\text{spatial mean})$	0.852	0.725	-0.633 – 2.336	1.175	0.250

428 Residual standard error: 0.171 on 28 degrees of freedom

429 Multiple R^2 : 0.785, Adjusted R^2 : 0.770

430 *F*-statistic: 51.06 on 2 and 28 DF, *P* value: 4.56e-10

431 Table S10. Summary of analyses of the relationship between \log_{10} (temporal mean) of density
 432 and \log_{10} (temporal variance) of density for the Fundamental simulation based on Fisher counts
 433 and the parameters estimated by the Yule-Walker method. Linear and quadratic models were
 434 fitted, and an analysis of covariance used “observed” or “simulated” as covariate.

435

436 Linear model (Taylor's law): $\text{lm}(\text{formula} = \log_{10}(\text{temporal variance}) \sim \log_{10}(\text{temporal mean}))$

437	Coefficients:	Estimate	SE	95%CI	<i>t</i> -statistic	<i>P</i> value
438	(Intercept)	-0.246	0.143	-0.531 – 0.039	-1.718	0.672
439	\log_{10} (temporal mean)	2.297	0.175	1.950 – 2.645	13.150	< 2.0e-16

440 Residual standard error: 0.289 on 83 degrees of freedom

441 Multiple R^2 : 0.676, Adjusted R^2 : 0.672

442 *F*-statistic: 172.9 on 1 and 83 DF, *P* value: < 2.2e-16

443 -----

444 Quadratic model: $\text{lm}(\text{formula} = \log_{10}(\text{temporal variance}) \sim \text{I}(\log_{10}(\text{temporal mean})^2) +$
 445 $\log_{10}(\text{temporal mean}))$

446	Coefficients:	Estimate	SE	95%CI	<i>t</i> -statistic	<i>P</i> value
447	(Intercept)	-0.891	0.442	-1.769 – -0.012	-2.016	0.047
448	$\log_{10}(\text{temporal mean})^2$	-1.055	0.685	-2.416 – 0.307	-1.541	0.128
449	\log_{10} (temporal mean)	3.399	1.111	1.778 – 6.199	3.589	0.0006

450 Residual standard error: 0.286 on 82 degrees of freedom

451 Multiple R^2 : 0.685, Adjusted R^2 : 0.677

452 *F*-statistic: 89.08 on 2 and 82 DF, *P* value: < 2.2e-16

453 -----

454 Analysis of covariance: simulated \log_{10} (temporal variance) and observed \log_{10} (temporal
455 variance) as a single vector as a linear function of simulated \log_{10} (temporal mean) and observed
456 \log_{10} (temporal mean) as a single vector, observed/simulated (o/s), and their interaction

457 Model: $\text{lm}(\text{formula} = \log_{10}(\text{temporal variance}) \sim \log_{10}(\text{temporal mean}) * \text{o/s})$

458	Coefficients:	Estimate	SE	95%CI	<i>t</i> -statistic	<i>P</i> value
459	(Intercept)	0.282	0.153	1.778 – 6.199	1.844	0.067
460	\log_{10} (temporal mean)	1.602	0.175	1.778 – 6.199	9.166	2.2e-16
461	o/s	-0.528	0.193	1.778 – 6.199	-2.738	0.007
462	\log_{10} (temporal mean):o/s	0.695	0.226	1.778 – 6.199	3.076	0.002

463 Residual standard error: 0.237 on 166 degrees of freedom

464 Multiple R^2 : 0.675, Adjusted R^2 : 0.669

465 *F*-statistic: 114.8 on 3 and 166 DF, *P* value: 2.2e-16

466

467 Table S11. Summary of analyses of the relationship between \log_{10} (temporal mean) of density
 468 and \log_{10} (temporal variance) of density for the Synchronized e_t simulation based on Fisher
 469 counts and the parameters estimated by the Yule-Walker method. SD was adjusted by the
 470 following equation: adjusted $SD_j = \text{estimated } SD_j - 0.065 \times \log_e(\text{estimated temporal mean})$.
 471 Linear and quadratic models were fitted, and an analysis of covariance used “observed” or
 472 “simulated” as covariate.

473

474 Linear model (Taylor's law): $\text{lm}(\text{formula} = \log_{10}(\text{temporal variance}) \sim \log_{10}(\text{temporal mean}))$

475 Coefficients:	Estimate	SE	95%CI	<i>t</i> -statistic	<i>P</i> value
476 (Intercept)	-0.012	0.138	-0.287 – 0.263	-0.085	0.933
477 \log_{10} (temporal mean)	1.794	0.172	1.452 – 2.134	10.458	< 2.2e-16

478 Residual standard error: 0.269 on 83 degrees of freedom

479 Multiple R^2 : 0.569, Adjusted R^2 : 0.563

480 *F*-statistic: 109.4 on 1 and 83 DF, *P* value: < 2.2e-16

481 -----

482 Quadratic model: $\text{lm}(\text{formula} = \log_{10}(\text{temporal variance}) \sim \text{I}(\log_{10}(\text{temporal mean})^2) +$
 483 $\log_{10}(\text{temporal mean}))$

484 Coefficients:	Estimate	SE	95%CI	<i>t</i> -statistic	<i>P</i> value
485 (Intercept)	-0.828	0.488	-1.799 – 0.143	-1.696	0.094
486 $\log_{10}(\text{temporal mean})^2$	-1.292	0.742	-2.767 – 0.184	-1.742	0.085
487 \log_{10} (temporal mean)	3.895	1.218	1.471 – 6.318	3.197	0.002

488 Residual standard error: 0.266 on 82 degrees of freedom

489 Multiple R^2 : 0.584, Adjusted R^2 : 0.574

490 *F*-statistic: 57.55 on 2 and 82 DF, *P* value: 2.426e-16

491 -----

492 Analysis of covariance: simulated \log_{10} (temporal variance) and observed \log_{10} (temporal
493 variance) as a single vector as a linear function of simulated \log_{10} (temporal mean) and observed
494 \log_{10} (temporal mean) as a single vector, observed/simulated indicator (o/s), and their interaction
495 : $\text{lm}(\text{formula} = \log_{10}(\text{temporal variance}) \sim \log_{10}(\text{temporal mean}) * \text{o/s})$

496 Coefficients:	Estimate	SE	95%CI	<i>t</i> -statistic	<i>P</i> value
497 (Intercept)	0.282	0.145	-0.005 – 0.569	1.939	0.054
498 \log_{10} (temporal mean)	1.602	0.166	1.274 – 1.930	9.637	< 2.2e-16
499 os	-0.294	0.186	-0.661 – 0.073	-1.580	0.116
500 \log_{10} (temporal mean): o/s	0.192	0.220	-0.242 – 0.625	0.873	0.384

501 Residual standard error: 0.225 on 166 degrees of freedom

502 Multiple R^2 : 0.649 Adjusted R^2 : 0.642

503 *F*-statistic: 102.1 on 3 and 166 DF, *P* value: < 2.2e-16

504

505 Table S12. Summary of analyses of the relationship between $\log_{10}(\text{spatial mean})$ of density and
 506 $\log_{10}(\text{spatial variance})$ of density for the Synchronized e_t simulation based on Fisher counts and
 507 the parameters estimated by the Yule-Walker method. SD was adjusted by the following
 508 equation: adjusted $SD_j = \text{estimated } SD_j - 0.065 \times \log_e(\text{estimated temporal mean})$. Linear and
 509 quadratic models were fitted, and an analysis of covariance used “observed” or “simulated” as
 510 covariate.

511

512 Linear model (Taylor's law): $\text{lm}(\text{formula} = \log_{10}(\text{spatial variance}) \sim \log_{10}(\text{spatial mean}))$

513	Coefficients:	Estimate	SE	95%CI	<i>t</i> -statistic	<i>P</i> value
514	(Intercept)	0.304	0.204	-0.112 – 0.721	1.493	0.146
515	$\log_{10}(\text{spatial mean})$	1.540	0.251	1.028 – 2.053	6.148	1.06e-6

516 Residual standard error: 0.186 on 29 degrees of freedom

517 Multiple R^2 : 0.566, Adjusted R^2 : 0.551

518 *F*-statistic: 37.8 on 1 and 29 DF, *P* value: 1.06e-6

519 -----

520 Quadratic model: $\text{lm}(\text{formula} = \log_{10}(\text{spatial variance}) \sim \text{I}(\log_{10}(\text{spatial mean})^2) + \log_{10}(\text{spatial mean}))$
 521 mean))

522	Coefficients:	Estimate	SE	95%CI	<i>t</i> -statistic	<i>P</i> value
523	(Intercept)	1.549	0.987	-0.473 – 3.571	1.569	0.128
524	$\log_{10}(\text{spatial mean})^2$	1.940	1.507	-1.146 – 5.026	1.288	0.208
525	$\log_{10}(\text{spatial mean})$	-1.611	2.459	-6.028 – 3.426	-0.655	0.518

526 Residual standard error: 0.184 on 28 degrees of freedom

527 Multiple R^2 : 0.590, Adjusted R^2 : 0.561

528 *F*-statistic: 20.16 on 2 and 28 DF, *P* value: 3.77e-06

529 -----

530 Analysis of covariance: simulated $\log_{10}(\text{spatial variance})$ and observed $\log_{10}(\text{spatial variance})$ as
531 a single vector as a linear function of simulated $\log_{10}(\text{spatial mean})$ and observed $\log_{10}(\text{spatial}$
532 mean) as a single vector, observed/simulated indicator (o/s), and their interaction

533 Model: $\text{lm}(\text{formula} = \log_{10}(\text{spatial variance}) \sim \log_{10}(\text{spatial mean}) * \text{o/s})$

534	Coefficients:	Estimate	SE	95%CI	<i>t</i> -statistic	<i>P</i> value
535	(Intercept)	0.549	0.110	0.329 – 0.769	4.989	5.85e-06
536	$\log_{10}(\text{spatial mean})$	1.242	0.128	0.986 – 1.498	9.725	8.64e-14
537	os	-0.245	0.224	-0.693 – 0.203	-1.093	0.279
538	$\log_{10}(\text{spatial mean}):\text{os}$	0.298	0.272	-0.245 – 0.842	1.099	0.276

539 Residual standard error: 0.178 on 58 degrees of freedom

540 Multiple R^2 : 0.702, Adjusted R^2 : 0.686

541 *F*-statistic: 45.48 on 3 and 58 DF, *P* value: 3.02e-15

Joel E. Cohen, Takashi Saitoh. 2016. Population dynamics, synchrony, and environmental quality of Hokkaido voles lead to temporal and spatial Taylor's laws. *Ecology*

Raw data, parameter estimates, and WinBUGS code for Bayesian analysis

Authors

Joel E. Cohen

Laboratory of Populations, The Rockefeller University and Columbia University; also Department of Statistics, Columbia University, and Department of Statistics, University of Chicago

1230 York Ave., Box 20

New York, NY 10065-6399, USA

cohen@rockefeller.edu

Takashi Saitoh

Field Science Center, Hokkaido University

North-11, West-10, Sapporo 060-0811, Japan

tsaitoh@fsc.hokudai.ac.jp

File list (files found within DataS1.zip)

`App1RawCountsOfVoles.csv`

`App2TrappingEffortTrapNights.csv`

`App3BayesCountsParameterEstimates.csv`

`App4SpatialMeanVarianceByYear.csv`

`App5WinBUGSCodeBayesianAnalysis.txt`

Description

`App1RawCountsOfVoles.csv`

Raw data: the total number of trapped voles, in a $T \times N$ matrix with $T = 31$ rows, one for each year $t = 1962, 1964, \dots, 1992$, and $N = 85$ columns $j = 1, 2, \dots, 85$, one for each ranger office

App2TrappingEffortTrapNights.csv

Raw data: amount of trapping effort (trap-nights), in the same format as Appendix S1

App3BayesCountsParameterEstimates.csv

Bayesian estimates of the density and the Gompertz parameters for each population at each survey and location using WinBUGS. For each population j , 11 additional rows at the bottom give: the temporal mean $m_j = (\sum_{t=1962}^{1992} N_{t,j})/T$ in the logarithm to the base 10, the temporal variance in the logarithm to the base 10, the Bayesian estimate of $a_{1,j}$, the Bayesian estimate of $a_{2,j}$, the Bayesian estimate of the standard deviation SD_j of the normal error term in the Gompertz model, latitude and longitude (in degrees and decimal fractions of degrees) of locations of the study sites; the Yule-Walker estimate of $a_{1,j}$, the Yule-Walker estimate of $a_{2,j}$, the Yule-Walker estimate of the standard deviation SD_j of the normal error term in the Gompertz model, and the Adjusted SD (see text for method of calculating Adjusted SD).

App4SpatialMeanVarianceByYear.csv

Logarithm to the base 10 of the spatial mean ($m_t = (\sum_{j=1}^{85} N_{t,j})/N$) and spatial variance (for 85 vole populations) of Bayes population density in each year.

App5WinBUGSCodeBayesianAnalysis.txt

WinBUGS code for Bayesian analysis of counts and trapping effort
